Supplementary Information: This Supplementary Information has not been peer reviewed. Title: The Sound of Resilience? Exploring trophic cascades and positive feedbacks between cod and eelgrass in a trawl-free ecosystem

Contents

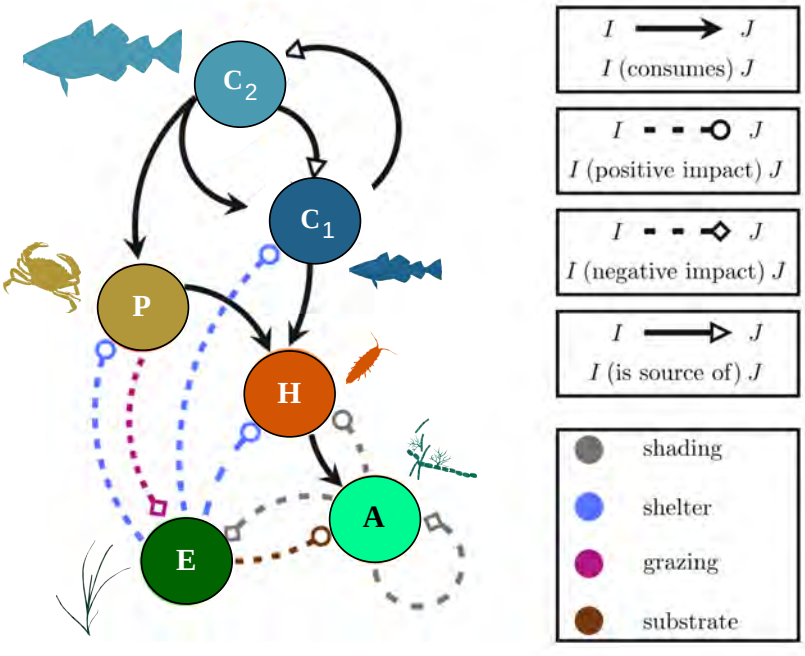

Figure S 1: **Schematic diagram of the interactions between the different trophic levels considered in the mathematical model**. The model considers five different trophic levels: adult (C_2) and juvenile (C_1) cod; mesopredators (P); mesoherbivores (H); eelgrass (E); and filamentous algae (A). Here, the solid arrows with black arrowheads denote predator-prey interactions, and solid arrows with white arrowheads denote transitions from adults to juveniles (via larvae production, not explicitly considered) and from juveniles to adults. Negative and positive interactions that do not constitute predator-prey interactions are shown with dashed arrows and colors. See Eqs. (1.2)-(1.6) for full details on the model interactions and Table S2 for parameter values.

1 Mathematical model

The model is designed to capture the essential trophic interactions structuring the ecosystem in eelgrass meadows in The Sound, with a focus on the dominant species and functional groups across multiple trophic levels. The framework aims to provide a mechanistic understanding of the system's dynamics while maintaining tractability by avoiding species-specific population details. Specifically, we consider as variables the population of cod $C(t)$ (predatory fish), mesopredators $P(t)$, mesoherbivores $H(t)$, eelgrass $E(t)$, and filamentous algae $A(t)$. The population of cod is divided into two age/size classes, including juveniles (C_1) ($\leq$ 25 cm) and adults (C_2) (>25 cm). Cod eggs and larvae are not explicitly modelled. Instead, they are implicitly included in the growth term of the equation for juvenile cod, as the model operates on a characteristic time scale of one year, and the hatching of eggs takes a few weeks [33] and the maturation of larvae to juveniles occurs within a few months [20, 21].

The equations governing the dynamics of each trophic level have the same basic structure for variable J, with $J \geq 0$ for $J \in \{C_1, C_2, P, H, E, A\}$, given by:

$$\frac{dJ}{dt} = \underbrace{g_J(t, J; \dots)}_{\text{growth}} - \underbrace{h_J(t, J; \dots)}_{\text{decay}} .$$

Figure S1 shows a schematic diagram of the main interactions considered among the trophic levels (see also Figure 2 in the main manuscript).

The model, which consists of six coupled ordinary differential equations (ODEs), is given by

Cod adults (C_2):

$$\frac{dC_2}{dt} = \underbrace{\frac{\alpha_{C_2C_1}\alpha_{C_1H}\Theta_{C_1H}(E,A)\ H}{1+\Theta_{C_1H}(E,A)\ \tau_{C_1H}\ H}\ C_1}_{\substack{\text{adult cod from juvenile}\\ \text{maturation} \sim \text{to } H \text{ consumption}}} - \underbrace{\nu_{C_2}\ C_2}_{\substack{\text{natural}\\ \text{mortality}}} - \underbrace{\eta_{C_2}\ C_2}_{\substack{\text{fishing}\\ \text{mortality}}} - \underbrace{\kappa_{C_2C_2}\ C_2^2}_{\substack{\text{intra-specific}\\ \text{competition}}}. \tag{1.1}$$

Cod juveniles (C_1):

$$\begin{aligned}\frac{dC_1}{dt} = \underbrace{\chi_{L\to 1}}_{\substack{\%\text{ larvae}\\ \text{to juveniles}}} \Bigg(\underbrace{\frac{\alpha_{C_LC_1}\ \Theta_{C_2C_1}(E)\ C_1 + \alpha_{C_LP}\ \Theta_{C_2P}(E)\ P}{1+\Theta_{C_2C_1}(E)\ \tau_{C_2C_1}\ C_1 + \Theta_{C_2P}(E)\ \tau_{C_2P}\ P}\ C_2}_{\substack{\text{larvae produced from adult cods} \sim \text{to}\\ \text{consumption of } C_1 \text{ and } P}} + \underbrace{\alpha_{C_Lh}\ \psi\ C_2}_{\substack{\text{larvae produced from adult}\\ \text{cod} \sim \text{to consumption of herring}}} \Bigg) - \underbrace{\frac{\alpha_{C_1H}\,\Theta_{C_1H}(E,A)\ H}{1+\Theta_{C_1H}(E,A)\ \tau_{C_1H}\ H}\ C_1}_{\substack{\text{juveniles maturing to}\\ \text{adult cod} \sim \text{to } H \text{ consumption}}}\\ - \underbrace{\nu_{C_1}C_1}_{\substack{\text{natural}\\ \text{mortality}}} - \underbrace{\eta_{C_1}\ C_1}_{\substack{\text{fishing}\\ \text{mortality}}} - \underbrace{\kappa_{C_1C_1}C_1^2}_{\substack{\text{intra-specific}\\ \text{competition}}} - \underbrace{\kappa_{C_1P}\ C_1\ P}_{\substack{\text{inter-specific}\\ \text{competition}}} - \underbrace{\frac{\Theta_{C_2C_1}(E)\ C_1}{1+\sum\limits_{J\in\{C_1,P\}}\Theta_{C_2J}(E)\ \tau_{C_2J}\ J}\ C_2}_{\substack{\text{mortality due to predation}\\ \text{by adult cod}}}.\end{aligned} \tag{1.2}$$

Mesopredators (P):

$$\frac{dP}{dt} = \underbrace{\frac{\alpha_{PH}\ \Theta_{PH}(E,A)\ H}{1+\Theta_{PH}(E,A)\ \tau_{PH}\ H}\ P}_{\substack{\text{mesopredator reproduction}\\ \sim \text{to } H \text{ consumption}}} - \underbrace{\nu_P\ P}_{\substack{\text{natural}\\ \text{mortality}}} - \underbrace{\kappa_{PP}\ P^2}_{\substack{\text{intra-specific}\\ \text{competition}}} - \underbrace{\kappa_{PC_1}\ P\ C_1}_{\substack{\text{inter-specific}\\ \text{competition}}} - \underbrace{\frac{\Theta_{C_2P}(E)\ P}{1+\sum\limits_{J\in\{P,C_1\}}\Theta_{C_2J}(E)\ \tau_{C_2J}\ J}\ C_2}_{\substack{\text{mortality due to predation}\\ \text{by adult cod}}}. \tag{1.3}$$

Mesoherbivores (H):

$$\frac{dH}{dt} = \underbrace{\frac{\alpha_{HA}\theta_{HA}\,A}{1+\theta_{HA}\,\tau_{HA}\,A}\,H}_{\substack{\text{mesoherbivore reproduction}\\ \sim \text{ to } A \text{ consumption}}} - \underbrace{\nu_H\,H}_{\substack{\text{natural}\\ \text{mortality}}} - \underbrace{\kappa_{HH}\,H^2}_{\substack{\text{intra-specific}\\ \text{competition}}} - \underbrace{\frac{\Theta_{PH}(E,A)\,H}{1+\Theta_{PH}(E,A)\,\tau_{PH}\,H}\,P}_{\substack{\text{mortality due to predation}\\ \text{by mesopredators}}} - \underbrace{\frac{\Theta_{C_1H}(E,A)\,H}{1+\Theta_{C_1H}(E,A)\,\tau_{C_1H}\,H}\,C_1}_{\substack{\text{mortality due to predation}\\ \text{by juvenile cod}}}. \tag{1.4}$$

Eelgrass (E):

$$\frac{dE}{dt} = \underbrace{\Gamma_E(A,N)\,E\left(1-\frac{E}{\omega_E\,k_E}\right)}_{\substack{\text{logistic growth from nutrient uptake}\\ \text{inhibited by shading by algae}\\ \text{and by nutrient-fuelled phytoplankton production}}} - \underbrace{\nu_E\,E}_{\substack{\text{natural}\\ \text{mortality}}} - \underbrace{\eta_E\,E}_{\substack{\text{eelgrass}\\ \text{destruction}}} - \underbrace{\theta_{AE}\,A\,E}_{\substack{\text{algae-induced}\\ \text{mortality}}} - \underbrace{\theta_{PE}\,P\,E}_{\substack{\text{mesopredator-}\\ \text{induced mortality}}}. \tag{1.5}$$

Filamentous algae (A):

$$\frac{dA}{dt} = \underbrace{\Gamma_A(A,N)\,A\left(1-\frac{A}{k_A+r_{EA}\,E}\right)}_{\substack{\text{logistic growth from nutrient uptake}\\ \text{inhibited by shading by algae}\\ \text{and by nutrient-fuelled phytoplankton production}}} - \underbrace{\frac{\theta_{HA}A}{1+\theta_{HA}\,\tau_{HA}\,A}H}_{\substack{\text{consumption by}\\ \text{mesoherbivores}}} - \underbrace{\nu_A\,A}_{\substack{\text{natural}\\ \text{mortality}}}. \tag{1.6}$$

The growth functions for eelgrass and filamentous algae are given by:

$$\Gamma_E(A,N) = \frac{\gamma_E+\gamma_{EN}\,N}{1+\xi_{EA}\,A}. \qquad \text{and} \qquad \Gamma_A(A,N) = \frac{\gamma_{AN}\,N}{1+\xi_{AA}\,A} \tag{1.7}$$

Above, k_E denotes the theoretical maximum carrying capacity for eelgrass (e.g., potentially favourable habitat in The Sound) and $\omega_E \in [0,1]$ the proportion of k_E that can actually be utilised. In identities (1.7), N denotes the concentration of nutrients in the water, which will be assumed to be constant (see Table S2 below).

The attack rate of predators are modelled through the functions

$$\begin{aligned} \Theta_{C_2 J}(E) &= \frac{\theta_{C_2 J}}{1 + w_{EJ}\, a(E)} , \qquad J \in \{C_1, P\} , \\ \Theta_{IH}(E, A) &= \frac{\theta_{IH}}{1 + w_{EH}\, a(E) + w_{AH}\, a(A)} , \qquad I \in \{C_1, P\} . \end{aligned} \tag{1.8}$$

Here, we consider $a(J) = J$, with $J \in \{E, A\}$, being $a(J)$ a term quantifying the sheltering effect in terms of abundance of J. That is, we assume that eelgrass diminishes the predator attack rates of adult cod on both mesopredators and cod juveniles, as well as that both eelgrass and filamentous algae provide shelter to mesoherbivores against the predation from mesopredators and cod juveniles.

1.1 Variables

Here we provide information on the variables corresponding to the key trophic levels considered in the model, together with their units and the initial values used (see Table S1 below).

	Description	Units	Initial conditions
t	time	year	—
C_2	adult cod	tonnes km^{-2}	0.182
C_1	juvenile cod	tonnes km^{-2}	0.05848
P	mesopredators	tonnes km^{-2}	10
H	mesoherbivores	tonnes km^{-2}	12
E	eelgrass	km^2	500
A	algae	tonnes km^{-2}	5

Table S1: Table of independent and dependent variables with the particular choice of units we use in the model. Note that, as a difference from the other variables, eelgrass units are given in (covered) area and not in biomass per area. This approach can be used because the processes tied to eelgrass mainly depend on the coverage (shelter, reduction of attack rates for species of the upper trophic levels, etc.). Eelgrass is not consumed in our model. The table also show initial conditions for each variable. For details on units and assumptions, see text below.

1.1.1 Initial conditions

- **Adult cod.** An average of 1.3 adult cod were caught per beach seine haul in eelgrass meadows in the Skagerrak region in June 2004, after subtracting juvenile cod from the total catch of 18.3 individuals per haul [50]. Since each beach seine haul samples approximately 500 m^2, this equates to an adult cod density of 0.0026 individuals m^{-2}. The adult cod had an estimated average length of 20 cm, corresponding to a mean weight of approximately 70 g based on established length–weight relationships (FishBase 2024: https://www.fishbase.se/search.php). This yields an estimated biomass of 0.000182 kg m^{-2} = 0.182 tonnes km^{-2} in these eelgrass habitats. While current cod densities in The Sound may differ, this should still give a plausible value for the density of adult cod in eelgrass meadows.

- **Juvenile cod.** An average of 17 juvenile cod were captured per beach seine haul in eelgrass meadows in the Skagerrak region [50] in June 2004. Given that a typical beach seine samples approximately 500 m^2, this equates to a density of 0.034 cod m^{-2}. This estimate aligns closely with values reported in similar habitats [37]. The mean total length of the juvenile cod was approximately 6 cm, which corresponds to an average individual weight of 1.72 g based on standard length-weight relationships [13]. This yields an estimated cod biomass of approximately 0.0000585 kg m^{-2} in eelgrass habitats [$(0.034 \times 1.72)/1000$]. That is, 0.05848 tonnes km^{-2}. Same as above, while current cod densities in The Sound may differ, this should still give a plausible value for the density of juvenile cod in eelgrass meadows

- **Mesopredators**. The amount of mesopredator fish (*Gobis niger*, *Gobiusculus flavescens*, *Gasterosteus aculeatus*, *Ctenolabrus rupestris*, *Symphodus melops*) caught in a beach seine in an eelgrass meadow in Skagerrak in June in 2004 [50] was $((4605.1 + 137.3 + 1781.7 + 62.8 + 2062.8)/500)/1000 = 0.017$ kg m^{-2} (500 m^2 equals area sampled by the beachseine, 1000 to get kg rather than g). As around 16 to 64 % of the mesopredator community is made up of crabs (derived from drop trap and beach seine surveys [2, 50]), this gives $0.017/(1-0.16)-0.017/(1-0.64)$ 0.02-0.05 kg wet weight m^{-2}, i.e. 20-50 tonnes km^{-2}. Same as above, while current mesopredator densities in The Sound may differ, this should still give a plausible value for the density of mesopredators in eelgrass meadows

- **Mesoherbivores.** [29] collected data on grazers from close to The Sound late summer/early autumn 2004. The site had ca. 2-6 g of ash-free dry weight of grazers m^{-2}. To translate this into kg wet weight, we used conversion factors from [18], where 0.12 seemed representative for the relevant taxa (amphipods, gastropods, decapods). This thus gives 50 tonnes km^{-2}.

- **Eelgrass.** Based on satellite mappings of shallow areas along the Swedish and Danish coast [5, 22] (see also https://marine-vegetation.satlas.dk//), around 987.0873 km^2 was classified as vegetation or soft bottoms, and was considered as suitable habitat for eelgrass. Of this area, around 50% was covered by vegetation (most of it likely eelgrass), i.e. around 500 km^2.

- **Algae.** Densities of filamentous algae have been measured to be ca. 1 g dry weight m^{-2} on the south coast of Sweden (close to The Sound) at the end of August and early September 2004 [29]. Based on published fresh weight: dry weight ratios from *Cladophora* and *Enteromorpha* [3, 35], we set the initial abundance of algae to 5 tonnes km^{-2}. These data were collected at quite an exposed site, so densities may be higher in other parts of The Sound.

1.2 Parameter values

Table S2 includes descriptions of model parameters and the values used. For some parameters (handling times, attack rates, nutrient concentration, herring densities, the direct impact of mesopredators

on eelgrass, reduction coefficients of attack rates, growth rates and carrying capacity of filamentous algae and natural mortalities), information on their derivation is provided after the table.

Table S 2: **Parameters of Eqs. (1.2)–(1.6).** The table shows the parameter (1st column), its ecological meaning (2nd column); its units (3rd column) with 1 meaning quantity is dimensionless; the possible cases found for each process: here I and J are live indices, i.e., in general $I, J \in \{C_1, C_2, P, H, E, A\}$ represent dependent variables (4th column); the used values (5th column); the ranges studied with the sensitivity analysis (6th column, see Section 3.2.6); and the references used to obtain or estimate these values (last column). The details about the estimated parameter values are described below and in Section 1.2. Superscript symbols direct to further information provided below the table.

Symbol	**Description**	**Units**	**Cases** (I, J)	**Estimated values**	**Estimated ranges**	**Ref.**
α_{IJ}	Energetic efficiency (biomass increase per biomass consumed)	1	(C_L, C_1)	$0.35^{\dagger}$	$[0.245, 0.455]$	[15]
			(C_L, P)	$0.35^{\dagger}$	$[0.245, 0.455]$	[15]
			(C_L, H)	$0.35^{\dagger}$	$[0.245, 0.455]$	[15]
			(C_2, C_1)	1^{*}	—	—
			(C_1, H)	0.25	$[0.175, 0.325]$	[40]
			(P, H)	0.23	$[0.161, 0.299]$	[40, 55]
			(H, A)	0.11	$[0.077, 0.143]$	[55]
ψ	Herring biomass	tonnes	—	6.521	$[4.565, 8.477]$	[11, 25, 47]
θ_{IJ}	Attack rate	$\frac{\text{km}^2}{\text{year tonnes}}$	(C_2, C_1)	0.54	$[0.378, 0.702]$	[14, 23, 31, 45]
			(C_2, P)	0.56	$[0.392, 0.728]$	[11, 14]
			(C_1, H)	1.06	$[0.742, 1.378]$	[9, 57]
			(P, H)	1.08	$[0.756, 1.404]$	[9, 57]
			(H, A)	2.30	$[1.610, 2.990]$	[9, 57]

Table 2 (continued)

	Description	Units	Cases (I, J)	Estimated values	Estimated ranges	Ref.
τ_{IJ}	Handling time	year	(C_2, C_1)	0.068	$[0.047, 0.088]$	[14, 23, 31, 46]
			(C_2, P)	0.052	$[0.0364, 0.0676]$	[11, 14]
			(C_1, H)	0.047	$[0.0329, 0.0611]$	[9, 57]
			(P, H)	0.031	$[0.0217, 0.0403]$	[9, 57]
			(H, A)	0.0294	$[0.0206, 0.0382]$	[9, 57]
$\chi_{L\to 1}$	Fraction of larvae transitioning to juveniles	year^{-1}	(C_L, C_1)	$0.295^{\bullet}$	$[0.2065, 0.3835]$	—
θ_{IE}	Negative impact on eelgrass	$\frac{\text{km}^2}{\text{year tonnes}}$	A	$0.001^{\$}$	$[0.0007, 0.0013]$	—
			P	0.0136	$[0.0095, 0.0177]$	[17, 42, 52]
r_{EA}	Carrying capacity per unit area of E	$\frac{\text{tonnes}}{\text{km}^4}$	—	0.5761	$[0.4033, 0.7489]$	[54]
γ_E	Intrinsic growth rate from sediment nutrients	year^{-1}	—	$1.5^{\blacklozenge}$	$[1.05, 1.95]$	—
γ_{IJ}	Growth rate from uptake of dissolved nutrients	$\text{km}^{-2}\,\text{year}^{-1}$	(E, N)	$0.568 \cdot 10^{-3}$	$[0.397, 0.738] \cdot 10^{-3}$	[49]
		$\frac{\text{km}^2}{\text{tonnes year}}$	(A, N)	$3.735^{\ddagger}$	$[2.615, 4.855]$	[41, 57]
ξ_{IJ}	Growth inhibition due to shading	$\frac{\text{km}^2}{\text{tonnes}}$	(E, A)	0.0049	$[0.0034, 0.0064]$	[4, 34, 53]
			(A, A)	0.0014	$[0.0010, 0.0018]$	[32]
k_I	Carrying capacity	$\frac{\text{tonnes}}{\text{km}^2}$	A	1325	$[927.5, 1722.5]$	[54]
		km^2	E	$987.0873^{@}$	—	—

Table 2 (continued)

	Description	**Units**	**Cases** (I, J)	**Estimated values**	**Estimated ranges**	**Ref.**
κ_{IJ}	Intraspecific and interspecific competition strength$^{\infty}$	$\frac{\text{km}^2}{\text{tonnes year}}$	(C_2, C_2)	10^{-3}	$[0.0007, 0.0013]$	—
			(C_1, C_1)	10^{-3}	$[0.0007, 0.0013]$	—
			(C_1, P)	10^{-3}	$[0.0007, 0.0013]$	—
			(P, C_1)	10^{-3}	$[0.0007, 0.0013]$	—
			(P, P)	10^{-3}	$[0.0007, 0.0013]$	—
			(H, H)	10^{-3}	$[0.0007, 0.0013]$	—
ν_I	Natural mortality	year^{-1}	C_2	0.201^{∇}	$[0.1407, 0.2613]$	[23]
			C_1	0.598^{∇}	$[0.4186, 0.7774]$	[23]
			P	0.22	$[0.176, 0.264]$	[44]
			H	0.99	$[0.693, 1.287]$	[56]
			A	14.61	$[10.227, 18.993]$	[12]
			E	$0.1^{\otimes}$	$[0.07, 0.13]$	[7]
N	Nutrient concentration	$\frac{\text{tonnes}}{\text{km}^3}$	—	5.742	$[4.0194, 7.4646]$	[1, 8]
η_I	Fishing mortality	year^{-1}	C_2	$\geq 0^{\perp}$	—	[23]
			C_1	$\geq 0^{\perp}$	—	[23]
η_E	Eelgrass external destruction rate	year^{-1}	—	$\geq 0^{\star}$	—	—

Table 2 (continued)

	Description	Units	Cases (I, J)	Estimated values	Estimated ranges	Ref.
w_{IJ}	Reduction coefficient of attack rate	km^{-2}	(E, C_1)	$1.087 \cdot 10^{-3}$	$[0.761, 1.413] \cdot 10^{-3}$	[38]
		km^{-2}	(E, P)	$1.087 \cdot 10^{-3}$	$[0.761, 1.413] \cdot 10^{-3}$	[38]
		km^{-2}	(E, H)	$2.006 \cdot 10^{-3}$	$[1.404, 2.608] \cdot 10^{-3}$	[16, 39]
		$\frac{\text{km}^2}{\text{tonnes}}$	(A, H)	10^{-3}	$[0.0007, 0.0013] \cdot 10^{-3}$	[51]
ω_E	Available habitat for eelgrass	1	—	$\leq 1^{**}$	$[0.7, 1]$	—

Explanatory notes to Table S2

†Research on bioenergetic modeling for Western Baltic cod took values of net conversion efficiency of 0.35 [15]. Notice that C_L, albeit not considered as a variable, refers to cod larvae.

*This value is set to 1 because we model the transition from cod juveniles to adults to be proportional to the consumption of mesoherbivores.

•This value has been estimated from the simulations with the fixed values of the table (without considering cod fishing and with $\omega_E = 1$ and $\eta_E = 0$) to obtain a mean population of juvenile cod of ≈ 0.058 along 75 years (as fixed in Table S1).

$Negative direct impact from algae suffocating eelgrass is assumed to be one order of magnitude lower than the impact of mesopredators on eelgrass.

♦Eelgrass can take up nutrients from both the overlying water column (through leaf blades) and interstitial sediment pore water (through roots) [19, 48]. The main nutrients for eelgrass growth, e.g., $NH4^+$ and PO_4^{3-}, are much more concentrated in sediment pore water than in the water column. Hence, sediments are often considered the main source of nutrients for eelgrass growth [36].

‡The growth rate of the algae due to the uptake of dissolved nutrients is much larger than the growth of eelgrass from the nutrients of the water column, as the eelgrass get most of their nutrients through their roots [36].

@Area obtained from satellite data. See Section 1.1.1

∞Since these values are difficult to parameterise based on available literature and data, we assume low values for both intraspecific and interspecific competition.

∇The natural mortality for adult and juvenile cod is based on estimates from the stock assessment [23].

The estimated instantaneous mortality of age $2-7+$ cod in the western Baltic stock was estimated to be in the range (0.201 0.411); the annual mortality of juvenile cod (age 1) was estimated

− to be 0.598. These parameters are also varies in our simulations to explore the impact on the dynamics of the ecosystem.

⊗The natural mortality of eelgrass has been set to the same order of magnitude provided by [7].

⊥This parameter will be explored to evaluate the impact of fishing on cod populations. Following available estimates from the Western Baltic stock we consider that the fishing mortality of juvenile cod is 12.807-fold lower than for adult cod [23].

⋆This parameter is left free to evaluate the impact of external eelgrass destruction on the dynamics.

**This parameter is normalised to 1, meaning that when $\omega_E = 1$, the 100% of the substrate where eelgrass can grow is in a good state and can be occupied by eelgrass meadows. This parameter was varied to evaluate the impact of available eelgrass habitat on the dynamics.

1.2.1 Maximum consumption rates, handling times, and attack rates

Rates of consumption for unlimited prey abundance, denoted as C_{IJ}^{max}, can be obtained from the literature for all the trophic levels in our model. This is not the case for the predation parameters of our model, namely the handling times τ_{IJ} and attack rates θ_{IJ}. Thus, we try to estimate these parameters using the Holling Type II functional response:

$$C = \frac{\theta_{IJ} J}{1 + \theta_{IJ}\tau_{IJ} J}.$$

Maximum consumption rates represent the functional response at high prey densities, when predator feeding is limited solely by handling time. In the limit $J \to \infty$, handling times can be inferred directly from the literature values of maximum consumption rates:

$$C_{IJ}^{max} = \frac{1}{\tau_{IJ}}. \tag{1.9}$$

As such, the handling times in Table S2 τ_{IJ} follow directly from the literature values of maximum consumption rates under the assumption of a Holling Type II response, and the results are listed in Table S3. However, θ_{IJ} parameterises at which prey density the maximum consumption is reached, so that additional assumptions are needed to estimate this value. In particular, one needs to relate a certain level of prey density to a consumption rate. We searched for empirical studies, however for the interactions that we model, no results could be found.

Therefore, as a first estimate, we use the initial conditions of the prey densities as used in the simulations (see Table S1) and assume that the consumption rates corresponding to these prey abundances are $1/K$th of their maximal values. Using this assumption, and fixing the value of K, one can compute the attack rate as:

$$\theta_{IJ} = \frac{1}{J^{IC}\tau_{IJ}(K-1)}.$$

We assume that the consumption curve for algae is near saturation, i.e., $K = 1+\epsilon$. For upper trophic levels, we set the attack rates to be of the same order of magnitude and assume higher coefficients K as the fish and crustaceans are not as abundant.

Interaction	Maximum consumption rate	Handling time	Attack rate	References
$C_2 \to C_1$	$[8, 17]$	$[0.058, 0.125]$	$[0.50, 2.0]$	[14, 23, 31, 45]
$C_2 \to P$	$[16, 35]$	$[0.029, 0.063]$	$[0.53, 1.16]$	[11, 14]
$P \to H$	$[2, 63]$	$[0.029, 0.063]$	$[0.07, 2.10]$	[9, 57]
$H \to A$	$[17, 51]$	$[0.020, 0.059]$	$[0.05, 4.55]$	[9, 57]

Table S3: Maximum consumption rates, handling times and attack rates from the literature used to estimate handling times and attack rates.

Ranges for maximum consumption rates follow from following publications:

- $\mathbf{C_{C_2C_1}}$: The maximum daily intake for adult cod feeding on juvenile cod is estimated from Refs. [30, 45].

$$C_{C_2 J} = 0.223\ \epsilon_J^{(0.104\,T - 0.000112\,T^3)}\ W^{0.802}. \tag{1.10}$$

  T denotes the temperature, ϵ_J the energy density of the prey J, and W the adult cod weight.

  The average temperature T in The Sound is 9.72 ± 0.24°C [31], the energy density of the prey juvenile cod ϵ_{C_1} is 4 kJ g^{-1} [45]. The body weight of adult cod W is estimated to be 234 -

9171 g [23]. In order to match the characteristic scale of a year, the daily rate is converted to the annual rate by a multiplication with 365.25, as adult cod feed on juveniles throughout the whole year [14].

- $\mathbf{C_{C_2P}}$: The same function is used to compute the maximum consumption rate of adult cod with mesopredators as a prey. The energy density of the mesopredators ϵ_P is assumed to be 2 kJ g^{-1}, which is the value for crabs [11]. Adult cod consumption on mesopredators is assumed to be present throughout the year, which is the case for at least the shore crabs and gobiids [11, 14].

- $\mathbf{C_{PH}}$: A black goby of 4-12 cm weighs ca. 0.75-22 g [13] and consumes a maximum of 10 gammarids of ca 10 mm per day [57], which corresponds to a weight of around 0.26 g daily consumption [9]. The maximum daily consumption rate is computed by dividing the intake by the average goby mass. For computing the annual value we multiply this by 182.625, as mesopredators only spend ca. half of the year in shallow habitats, where mesoherbivores are present [52].

- $\mathbf{C_{C_1P}}$: The maximum consumption of juvenile cod feeding on mesopredators is assumed to be the same as above for mesopredators on herbivores.

- $\mathbf{C_{HA}}$: A 10 mm gammarid consumes a maximum of 0.0049 g of algae per day [57], and weighs ca. 0.026 g [9]. The resulting daily consumption rate is multiplied by 182.625 days, as gammarids are assumed to feed on algae during half of the year.

1.2.2 Nutrient concentration

The nominal value of the nutrient concentration in The Sound is 0.41 μM , and we consider a relatively wide range of [0.38, 1.36] μM [1, 8, 41, 49, 60], equivalent to $[5.323, 19.0492]$ tonnes km^{-3}. For the conversion of units to mass concentration 1 μg N l^{-1} = 0.071394 μmol l^{-1} is used [28].

1.2.3 Herring population

The presence of herring in The Sound shows a strong seasonal pattern [11]. When averaged across months, this gives an estimate of ca. 45 000 tonnes of herring, based on surveys conducted in the mid-1990s [47]. Based on the most recent stock assessment, the stock is now at ca. 30% of the estimated stock size in the mid-1990s [25] thus corresponding to ca. 13 000 tonnes. Divided by the area of The Sound (ca. 2300 km^2), this gives an estimate of ca. 6.521 tonnes km^{-2}.

1.2.4 Mesopredators' impact on eelgrass

In addition to the impacts acting via indirect top-down control, shore crabs have a direct negative effect on eelgrass by tearing off shoots and predating on the seeds [17, 27]. Around 16 to 64 % of the mesopredator community in these areas is made up of crabs (derived from drop trap and beach seine surveys [2, 50]). Accounting for the proportion of crabs we estimate that 0.01 to 0.072 of initial eelgrass is removed per kg m^{-2} mesopredators per day [17], the daily instantaneous rate of removal is then $\theta_{PE}^{daily} = -\ln(1-(0.01-0.072)\ \text{day}^{-1}\ (\text{kg m}^{-2})^{-1}$, as the crabs are absent ca. half of the year the yearly instantaneous rate is computed as $\theta_{PE} = \theta_{PE}^{daily} \cdot \frac{365}{2} \cdot 10^{-3} \cdot \text{year}^{-1} \cdot \frac{\text{tonnes}}{\text{km}^2}^{-1}$, where the factor 10^{-3} reflects only the conversion of the units for the density of mesopredators, i.e. from the negative impact rate per kg m^{-2} to per tonnes km^{-2} of mesopredators.

1.2.5 Reduction coefficients of attack rates

- w_{E,C_1}: A study found that attack rates on juvenile cod from a variety of predators are 3-4 times higher in unvegetated sites compared to the rates in eelgrass meadows, after standardising by predator abundance [38].

  For $E = 0$, the attack rate function 1.8 should be equal the parameter value $\theta_{C_2C_1}$, and the value should be 3 to 4 times lower for the case that the whole region of The Sound (≈ 2300 km^2) is covered with vegetation. For $E = k_E$, with $a(E) = E$ we get $w_{E,C_1} = [2/A_{The\ Sound}, 3/A_{The\ Sound}] = [0.870, 1.304] \cdot 10^{-3}$. The midpoint is then $1.087 \cdot 10^{-3}$.

- $w_{E,P}$: We assume that vegetation has the same effect on the attack rates on mesopredators as on juvenile cod.Therefore for the reduction coefficient we have $w_{E,P} = [2/A_{TheSound}, 3/A_{TheSound}] = [0.870, 1.304] \cdot 10^{-3}$.

- $w_{E,H}$: The attack rates on mesoherbivores by stickleback and juvenile cod have been found to be 1-10 times higher in unvegetated areas compared to in eelgrass meadows [16, 39]. For the upper boundary we have $9/2300 = 3.913 \cdot 10^{-3}$, for the lower boundary we take 10^{-4}, for considering a small effect. The midpoint $2.006 \cdot 10^{-3}$ is used as the nominal value.

- $w_{A,H}$: The attack rate on mesoherbivores by juvenile cod is reduced 1.3-6 times in algae covered areas [51]. As the algae concentration is measured in density, not in area, there is no natural upper limit like the area of The Sound as in the case of eelgrass, and we here therefore use the carrying capacity of algae in eelgrass meadows to represent an algae-covered area ($k_{A,max}$ 2650 tonnes km^{-2}). Thus we have $w_{AH} = [0.3\ k_{A,max}, 5\ k_{A,max}] = [0.113, 1.887] \cdot 10^{-3}$.

1.2.6 Growth rate of filamentous algae as a function of nutrient concentration

The growth rates of filamentous algae are 0.32 g $(\text{g} \cdot \text{day})^{-1}$ at 1.2 μM (≈ 0.0168 kg m^{-3}) and 0.85 g $(\text{g} \cdot \text{day})^{-1}$ at 4.9 μM (≈ 0.069 kg m^{-3}). Here, g $(\text{g} \cdot \text{day})^{-1}$ stands for the algae biomass produced, quantified in grams (g) per 1 g existing algae. Assuming 0 growth for the absence of nutrients in the water column followed by a linear increase, one gets the annual growth parameter:

$$\gamma_{AN} = \frac{0.85 - 0.32}{4.9 - 1.2} \cdot 365.25\ \text{year}^{-1}(\mu M)^{-1} = 3.735\ \text{year}^{-1}(\text{tonnes km}^{-3})^{-1}$$

1.2.7 Carrying capacity of filamentous algae

The carrying capacity for algae in eelgrass meadows is around 2650 tonnes km^{-2}, while in bare sediments, the algae coverage is known to decrease to $20 - 80\%$ of its maximum value [54].

We model the eelgrass-dependent carrying capacity as $k_A + r_{EA}E$ where k_A denotes the carrying capacity of algae on bare sediments; assuming that the algae coverage on bare sediments is 50% of maximum, we get a nominal value of $k_A = 1325$ tonnes km^{-2}.
The parameter r_{EA} denotes the increase in algae carrying capacity with eelgrass covered area E. The total area of The Sound is ≈ 2300 km^2. If the whole strait was covered with eelgrass (corresponding to $E = 2300$ km^2), the carrying capacity would be 2650 tonnes km^{-2}, from this we can compute the parameter r_{EA} as:

$$r_{EA} = \frac{k_{max} - k_A}{E_{max}} = \frac{(2,650 - 1,325)\,\text{tonnes km}^{-2}}{2,300\,\text{km}^2} = 0.5761\,\text{tonnes km}^{-4}$$

For The Sound, with the carrying capacity of eelgrass being 987.087 km^2, the maximum carrying capacity for algae accounts to 1893.648 tonnes km^{-2}.

1.2.8 Natural mortality

We assume a survival curve of type III, obtained from

$$\frac{dI}{dt} = -\nu_I I,$$

ν_I are the instantaneous mortality rates. We use two different ways of estimating these values, depending on the available literature. For the case that the daily instantenous mortality rates are known, the annual ones follow straightforwardly: $\nu_I^{annual} = 365.25 \cdot \nu_I^{daily}$. Otherwise, we use the information on the life spans that are related to the mortality rates as $T_I = 1/\nu_I$.

The natural mortality of the cod follow directly from the stock assessments [23], whereas for other trophic groups following values are used:

- Mesopredator natural mortality ν_P is computed using the lifespan of 3 to 6 years following [10, 44].
- Mesoherbivore *Gammarus pulex* has a lifespan of 350-450 days [56] this is used for estimating ν_H.
- Instantaneous daily mortality of algae is 0.04 [12], corresponding to a yearly rate of 14.61. This means that the lifespan of the filamentous algae is around 25 days.
- Lifespan of eelgrass shoots is about 1.5 years, i.e. 554.8 days according to [7]. This corresponds to an instantaneous annual mortality rate of 0.66.

1.3 Extinction thresholds

In our simulations, the abundance/density of each trophic level can achieve very low values, especially under fluctuating dynamics. These values are unlikely to represent viable populations, and therefore we here define extinction thresholds for each of the trophic levels, which we here take to be the density that corresponds to having only one individual of the groups C_1, C_2, P, H in the whole region of The Sound. Here, we calculate the minimum density per area in tonnes km^{-2} corresponding to one individual. Such extinction thresholds, labeled as ϵ_i with $i \in \{A, E, H, P, C_1, C_2\}$, are computed as follows:

- Juvenile cod (C_1): weighs $0.5 - 2$ kg, we take the lower limit.
- Adult cod (C_2): weighs 5-12 kg, we take the lower limit.
- Mesopredators (P): black goby of 4-12 cm weighs 0.75-22 g [13], we take again the lower limit.
- Mesoherbivores (H): *Gammarus locusta* weighs approximately 0.026 g. [9].

The extinction threshold for the filamentous algae ϵ_A is set to a low value, 10^{-12}. Similarly, the extinction of eelgrass will be assumed to take place with an area below the threshold $\epsilon_E = 10^{-12}$. The use of similar, low, threshold values (e.g., 10^{-9}, 10^{-10}, 10^{-11}) for eelgrass and algae does not alter the results obtained (results not shown).

Population	Weight per individual	Minimum density tonnes km^{-2}	Example species
C_1	0.5-2.0 (kg)	$\epsilon_{C_1} = 2.17 \cdot 10^{-7}$	*Gadus morhua*
C_2	5.0-12.0 (kg)	$\epsilon_{C_2} = 2.17 \cdot 10^{-6}$	*Gadus morhua*
P	0.75-22.0 (g)	$\epsilon_P = 3.26 \cdot 10^{-10}$	*Gobius niger*
H	0.026 (g)	$\epsilon_H = 1.13 \cdot 10^{-11}$	*Gammarus locusta*

Table S 4: Extinction thresholds. Table of weights per individual for each trophic level and the density that corresponds to having only one individual of the group in The Sound ($\approx$ 2,300 km^2).

1.4 Model assumptions and limitations

The model uses ordinary differential equations to describe yearly changes in key trophic levels of an eelgrass ecosystem in The Sound.

Several assumptions underlie the model. First, we assume homogeneous mixing of populations in space. No explicit spatial structure, migration, or metapopulation processes are considered, and species interactions are therefore represented by mass-action terms without accounting for local habitat heterogeneity or patchiness. Second, the model is deterministic and does not include demographic or environmental stochasticity; fluctuations in recruitment, mortality, or environmental forcing are neglected. Third, we assume a constant abiotic environment: nutrient concentrations and other physical conditions are held fixed, and the model does not resolve seasonal cycles or interannual variation in nutrient input, light availability, or temperature, despite their known influence on primary production and species interactions. Fourth, trophic levels are aggregated into single variables. For example, mesopredators or mesoherbivores combine several species with potentially distinct ecological roles and life histories. Similarly, cod are modeled in two life stages (juveniles and adults), while eggs and larvae are only implicitly represented through recruitment terms. Finally, interactions are simplified by assuming Holling type II functional responses, with parameter values drawn from empirical literature when available. Habitat-mediated effects of eelgrass and algae are included as reductions in attack rates, but other ecological processes such as recruitment facilitation or survival differences across microhabitats are omitted. These assumptions impose limitations on the scope of the results. The absence of spatial structure prevents the model from addressing habitat fragmentation, dispersal, or local refuge effects, which may strongly influence coastal ecosystem dynamics. Likewise, the lack of stochasticity and seasonal forcing means that variability driven by recruitment pulses, climate fluctuations, or anthropogenic disturbances is not captured. Aggregating species into trophic compartments may also obscure important interspecific differences, such as variation in predation pressure or resilience to environmental change. For these reasons, the quantitative results of the model, such as exact abundances or extinction times, should be interpreted with caution. The model is intended to provide qualitative insights into trophic interactions and to highlight possible nonlinear responses to perturbations.

However, given the important role that environmental fluctuations may play in the ecosystem, especially for apex species, we use the modeling framework to explore the impact of environmental noise on adult and juvenile cod populations. Although most results are obtained from a deterministic approach, we also examine how stochastic variations in cod natural mortality affect the dynamics of the entire trophic system. Particular emphasis is placed on the effects of these fluctuations on cod population dynamics.

In a nutshell, the model offers a tractable and ecologically grounded framework to explore the role of cod and eelgrass in structuring trophic interactions in The Sound. Its results are best in-

terpreted as qualitative scenarios and hypotheses rather than precise forecasts, and they should be complemented in future work by models that incorporate spatial heterogeneity, seasonal dynamics, and other stochastic processes.

2 Methods

2.1 Supplementary information for time series data analysis

The plots and tables below support the method description for the empirical data presented in the main text.

Year	**Quarter 1**				**Quarter 4**			
	21	22	23	24	21	22	23	24
2001	22	32	1	69	17	32	3	42
2002	25	28	3	55	26	20	4	46
2003	23	22	3	48	25	22	3	46
2004	25	22	4	50	24	21	3	47
2005	24	23	4	44	22	30	3	47
2006	23	25	4	43	23	23	3	45
2007	23	22	3	46	25	28	2	42
2008	25	37	3	35	24	31	2	47
2009	23	25	3	45	19	25	3	54
2010	24	34	3	51	23	33	3	31
2011	23	40	3	45	25	27	3	50
2012	25	25	3	53	26	24	3	47
2013	25	24	3	54	25	25	2	38
2014	24	28	3	50	24	25	3	49
2015	24	29	3	50	24	33	5	38
2016	25	34	5	52	23	40	5	53
2017	24	37	6	50	24	35	5	48
2018	24	39	5	53	28	38	5	42
2019	24	39	5	39	25	40	6	50
2020	19	43	5	57	25	40	5	51
2021	24	42	5	50	24	45	5	48
2022	25	50	5	50	25	49	5	53
2023	22	51	5	45	26	38	5	48
2024	27	42	5	48	25	42	5	51
2025	26	39	6	49				

Table S 5: Number of hauls from each ICES sub-division per year in each quarter (1 = February-March, 4 = October-December) as part of the Baltic International Trawl Survey. Data were only included when at least three hauls were available in a given sub-division in a given year within each quarter (those not included are coloured grey).

Year	The Sound	Kattegat	
	Barsebäck	Kullen	Ringhals
sub-loctions	Barsebäcksverket, Tjuvakroken, Barsebäckshamn, Sjöbobadet/Golfbanan and Lundåkrabukten. Some stations at Barsebäck are located close to a previous outlet of cooling water from a nuclear reactor that was closed in 1999, but are considered to be unaffected over our study period [58].	No division into sub-locations.	We only included data from the sub-location Vendelsö. This is a reference area for the Ringhals power plant, and is unaffected by the cooling water [6, 59].
Sampling period	2002–2008: April and August; 2009–present: August	2002–2004: April, August and October; 2005–2012: August and October; 2013: no fishing; 2014–present: October	2002–2004: April, August and October; 2005–present: April and August
Stations	2002–2020: 3 stations per sub-location, except Lundåkrabukten that was fished with 6 stations; 2021–present: 70 stations (5 of the original stations were kept, and 65 new stations designated, to better represent the depth distribution of the area). Note that subsetting to depths 1.5-5.6 m removes some stations.	2002–2020: 60 stations; 2021–present: 70 stations (16 of the original stations were kept, while 54 new stations were designated, to better represent the depth distribution of the area). Note that subsetting to depths 1.5-5.6 m removes some stations.	6 stations.
Set-up	2002–2008: 12 nights per station per sampling period and year 2009–2020: 6 nights per station per year 2021–present: Each station fished one night per year.	2002–2020: For each fishing night (6 per year and sampling period), 15 randomly selected stations are fished, so that one station may be fished several times per year, while others are not fished at all. 2021–present: Each station fished one night per year.	Each station fished 9 times per sampling period.

Table S6: Description of the sampling set-up for each fyke net monitoring location that was included in our analyses. Note that we only used data from the first night of fishing and that for our analyses, we only used data up until 2020, before there was a change in the station used.

Year	The Sound	Kattegat	
	Barsebäck	Kullen	Ringhals
2002	36 (36)	162 (162)	18 (18)
2003	36 (36)	155 (155)	18 (18)
2004	36 (36)	152 (152)	18 (18)
2005	36 (36)	101 (101)	18 (18)
2006	36 (36)	104 (97)	12 (12)
2007	36 (36)	104 (104)	12 (12)
2008	36 (36)	103 (103)	12 (6)
2009	18 (18)	100 (100)	12 (12)
2010	18 (18)	102 (101)	12 (12)
2011	15 (15)	91 (91)	12 (12)
2012	18 (18)	99 (92)	12 (12)
2013	18 (18)	0 (0)	12 (12)
2014	18 (18)	47 (47)	12 (12)
2015	18 (18)	53 (53)	12 (12)
2016	18 (18)	48 (48)	12 (12)
2017	18 (18)	51 (51)	12 (12)
2018	21 (0)	51 (47)	12 (12)
2019	18 (0)	52 (52)	12 (12)
2020	18 (18)	50 (50)	12 (12)
2021	21 (0)	37 (0)	13 (0)
2022	22 (0)	37 (0)	12 (0)
2023	22 (0)	36 (0)	12 (0)
2024	0 (0)	36 (0)	0 (0)

Table S7: Total number of paired fyke nets deployed per year and location, in parentheses the number of samples included in the analyses, i.e. without missing temperature data and collected before the change in the stations fished (see Table S6). All data are included in the plots presented.

2.2 Numerical tools

The solutions of model given by Eqs. (1.2)-(1.6) have been obtained numerically by using an 8th order Runge-Kutta-Fehlberg method with automatic step size control and relative tolerance 10^{-15}.

2.3 Presence-abundance index, I_{PA}

We here define a structural index, labeled I_{PA}, which indicates the state of the ecosystem by combining a measure of the presence and abundances of the different trophic levels. This index, used to quantify presence and abundance (PA) of the different trophic levels in a given parametric region (i.e., computed in two-dimensional parameter domains D), is given by:

$$I_{PA} = \sum_{i=1}^{n} \delta_{i\epsilon_i} \bar{X}_i^D, \qquad i \in \{A, E, H, P, C_1, C_2\}, \tag{2.1}$$

where $0 \leq I_{PA} \leq n$, n being the total number of trophic levels considered for the computation of the index. $\delta_{i\epsilon_i}$ is a Heaviside step function, with

$$\delta_{i\epsilon_i} = \begin{cases} 1, & \text{if } \bar{X}_i^D > \epsilon_i, \\ 0, & \text{if } \bar{X}_i^D \leq \epsilon_i. \end{cases}$$

The $\delta_{i\epsilon_i}$ is the indicator function of whether $\bar{X}_i^D$ will exceed the extinction thresholds, ϵ_i (see Table S4). Moreover, $\bar{X}_i^D$ is the abundance of the trophic level i normalised in the studied domain. This index allows us to identify parameter regions with the highest I_{AP} values, i.e., maximum presence of trophic levels and maximum abundances of each level.

2.4 Four-parameter logistic model and fitting procedure

To describe and quantify the relationship between an ecological driver (e.g., fishing mortality of adult cod and eelgrass destruction rates) and cod population density, we employed a flexible four-parameter logistic model. This model is widely used in ecological and biological systems to represent nonlinear responses with saturation levels and threshold dynamics. It is defined as:

$$y(x) = A + \frac{L - A}{1 + \exp\big(k(x - x_0)\big)}, \tag{2.2}$$

where:

- x is a continuous ecological or anthropogenic parameter (here, fishing mortality and eelgrass destruction rate).
- $y(x)$ represents the mean abundance of a given trophic level (here, mean cod density including juveniles and adults).
- A is the lower asymptote, the minimum cod density under extreme or unfavorable parameter values.
- L is the upper asymptote, the maximum cod density achievable under optimal conditions.
- x_0 is the inflection point, the parameter value at which cod density is halfway between A and L, marking a critical ecological threshold.
- k is the steepness coefficient, describing how sharply cod density changes around the threshold.

This general parameterisation allows the function to represent cod population responses to various ecological or anthropogenic factors. In this study, x corresponds to eelgrass habitat degradation rate and fishing mortality, but the same formulation can be applied to other systems or environmental gradients.

Model parameters (A, L, x_0, and k) were estimated using a nonlinear least-squares optimisation implemented in Python (version 3.12.8), employing the `curve_fit` function from the `optimize` module of the SciPy library (version 1.13.1) [61]. Initial parameter values were chosen based on descriptive statistics: A was initialised to the minimum observed cod density, L to the maximum observed density, x_0 to the median of the predictor parameter (x), and k to a positive value to allow for steep transitions.

The optimisation minimised the residual sum of squares (RSS):

$$\mathrm{RSS} = \sum_{i=1}^{n} \left(y_i - y(x_i)\right)^2 ,$$

where y_i is the observed cod density at parameter value x_i. Model performance was evaluated using the coefficient of determination (R^2):

$$R^2 = 1 - \frac{\sum_{i=1}^{n} \left(y_i - y(x_i)\right)^2}{\sum_{i=1}^{n} \left(y_i - \bar{y}\right)^2},$$

where $\bar{y}$ is the mean observed cod density.

2.5 Stochastic dynamics: simulating environmental noise

To incorporate environmental stochasticity, we allowed selected model parameters to fluctuate around their deterministic mean-field values. For a generic parameter p, with deterministic value $\bar{p}$, the stochastic realization at time t was defined as

$$p(t) = \bar{p}\left(1 + \sigma\xi(t)\right),$$

where σ controls the amplitude of environmental fluctuations and $\xi(t)$ is a standard normally distributed random variable,

$$\xi(t) \sim \mathcal{N}(0, 1).$$

Thus, σ measures the strength of stochastic deviations relative to the deterministic value. When $\sigma = 0$, the deterministic model is recovered exactly, $p(t) = \bar{p}$.

In this study, environmental stochasticity was applied to the natural mortality rates of adult and juvenile cod. Specifically, at each stochastic update, the mortality rates were given by

$$\nu_{C2}(t) = \bar{\nu}_{C2}\left(1 + \sigma\xi_{C2}(t)\right),$$

$$\nu_{C1}(t) = \bar{\nu}_{C1}\left(1 + \sigma\xi_{C1}(t)\right),$$

where $\bar{\nu}_{C2}$ and $\bar{\nu}_{C1}$ are the deterministic mean-field mortality rates of adult and juvenile cod, respectively. The random variables $\xi_{C2}(t)$ and $\xi_{C1}(t)$ were independently sampled from a standard normal distribution.

Since mortality rates cannot be biologically negative, negative stochastic realizations were set to zero:

$$\nu_{Ci}(t) = \max\left\{0, \bar{\nu}_{Ci}\left(1 + \sigma\xi_{Ci}(t)\right)\right\}, \qquad i \in \{1, 2\}.$$

This formulation preserves the deterministic model as the baseline case and allows the intensity of environmental variability to be controlled through the single noise amplitude σ.

2.6 Sensitivity analysis: Monte Carlo method

Most of the parameter values were either derived or directly obtained from the literature, as reported in Table S2. To assess the robustness of our findings to uncertainty in the parameter estimates, we adopt a Monte Carlo approach. This method provides a straightforward yet powerful way to perform a sensitivity analysis, allowing us to quantify how uncertainties in parameterisation may propagate through the system and influence ecological outcomes.

To do so, we start from the reference values reported in Table S2, which were either directly derived or obtained from the literature. Each of these fixed reference values was perturbed by random sampling within a defined range. Specifically, for a given parameter with value v, we generated alternative realisations by drawing from a uniform distribution:

$$v_R \sim U\big(v \cdot (1-\mu),\ v \cdot (1+\mu)\big),$$

with $\mu = 0.3$. This means that for each parameter, the model was systematically explored within $\pm 30\%$ of its reference value (see Table S2 for ranges for each parameter). By applying this procedure across all relevant parameters simultaneously, we obtained a broad ensemble of randomised configurations of the system. This ensemble reflects plausible ecological variability and accounts for the uncertainty inherent in parameter estimation. Specifically, this randomised sensitivity framework enables us to test the consistency of our results against parameter uncertainty. In this way, the Monte Carlo sensitivity analysis provides an additional layer of validation and supports the generality of the conclusions derived from fixed-parameter simulations.

To obtain a continuous representation of the abundance distribution across parameter space, we employed a kernel regression smoother based on the Nadaraya–Watson estimator [43, 62]. Specifically, given sampled parameter values (x_i, y_i) with associated abundances z_i, the abundance at a grid point (x, y) was estimated as a kernel-weighted average:

$$\hat{z}(x,y) = \frac{\sum_{i=1}^{n} K_h(\|(x,y) - (x_i,y_i)\|)\ z_i}{\sum_{i=1}^{n} K_h(\|(x,y) - (x_i,y_i)\|)},$$

where $K_h(\cdot)$ is a Gaussian kernel with fixed bandwidth $h = 0.05$ and n is the number of sampled points. This procedure produces a smooth, continuous abundance surface that suppresses stochastic variability from random sampling while preserving large-scale spatial patterns. The smoothing was performed on an 80×80 grid spanning the parameter space, ensuring comparability across datasets. Hotspot regions were then identified as those exceeding a given quantile threshold of the smoothed distribution (e.g., the 90th percentile for the top 10% of values). Contour lines at the selected thresholds were overlaid on the abundance surface to delineate high-density or low-density regions. This percentile-based approach ensures a consistent and data-driven definition of hotspots, independent of the absolute scale of abundances [43]. Specifically, the contour lines for maximum abundances were applied to cod, mesoherbivores, and eelgrass. Contour lines for minimum abundances (lowest 10% values) were applied to mesopredators and filamentous algae. This representation of the randomised parameter ensembles has been used in Figs. S20-S24.

3 Results

In this section we first present some additional results from the time series obtained from trawl surveys, fyke nets, and eelgrass monitoring (Section 3.1). Then, we explore the dynamics of the mathematical model given by Eqs. (1.2)-(1.6). Specifically, we explore how perturbations on cod and eelgrass impact the other trophic levels. Specifically, for cod, we investigate the natural mortality for juvenile (ν_{C1}) and adult (ν_{C2}) cod as well as the fishing mortality of adult cod (η_{C2}) (assuming that the fishing mortality for juveniles η_{C1} is $\eta_{C2}/12.807$ [23]). For eelgrass, we explore two parameters:

(i) external destruction rate of eelgrass (η_E); and (ii) decrease in the area of suitable available area for eelgrass (ω_E). All the presented results have been obtained by solving the differential equations numerically (see Section 2.2).

First, we begin by computing phase diagrams in two-dimensional parameter spaces, illustrating how the mean abundances of the trophic levels change when tuning pairs of parameters simultaneously. These mean abundances are obtained by averaging the populations over 75-year simulations. For trophic levels whose abundances fall below the extinction thresholds defined in Section 1.3, the corresponding mean abundance is set to zero. Based on the two-dimensional abundance diagrams for each trophic level, we derive a structural index quantifying the combined presence and abundance of trophic levels, thus identifying parameter regions that maximise persistence and biomass (see Section 2.4). We compute the index for (i) all trophic levels and (ii) cod and eelgrass, the key levels linked to major ecosystem services.

Second, one-dimensional parameter analyses are performed to provide complementary insights into the effects of these parameters on mean population abundances (also averaged over 75-year simulations). Again, for trophic levels whose abundances fall below the extinction thresholds defined in Section 1.3, the corresponding mean abundance is set to zero.

Third, we analyse how extinction times respond to increasing eelgrass destruction and fishing mortality.

Fourth, and finally, we perform a sensitivity analyses to evaluate the robustness of these results (see Section 2.6).

3.1 Additional results from empirical time series data analysis

Below we display additional results from the time series obtained from trawl surveys, fyke nets, and eelgrass monitoring. For the discussion on these data see the main manuscript.

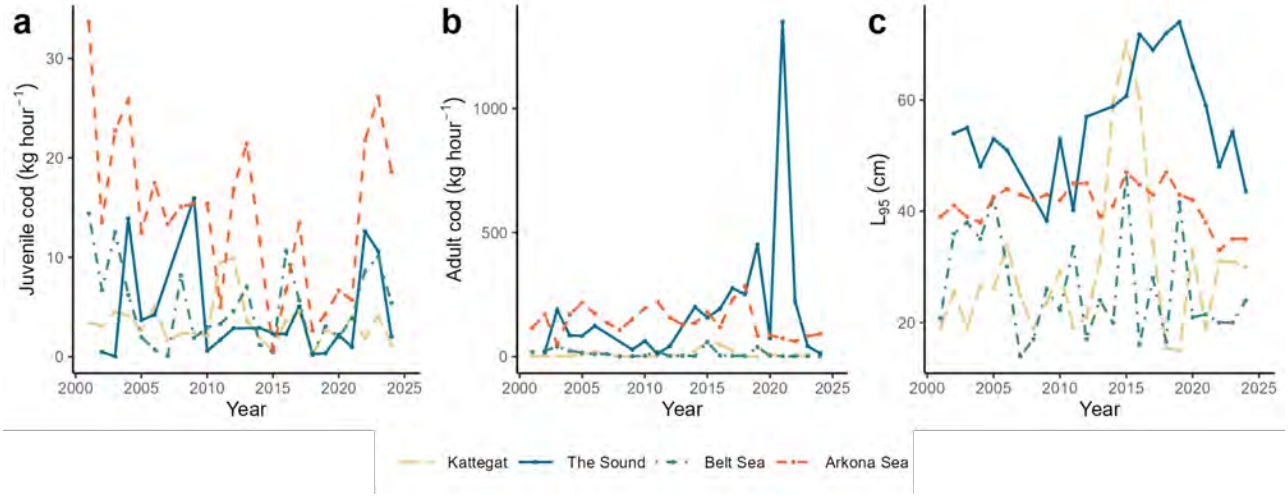

Figure S2: BPUE of (a) juvenile ($\leq$ 25 cm) and (b) adult (>25 cm) cod, and (d) the 95th percentile of total length of cod caught in trawl surveys in The Sound, the Kattegat, the Belt Sea and the Arkona Sea in Quarter 4. For corresponding plot for Quarter 1 see Figure 3a-c in the main text.

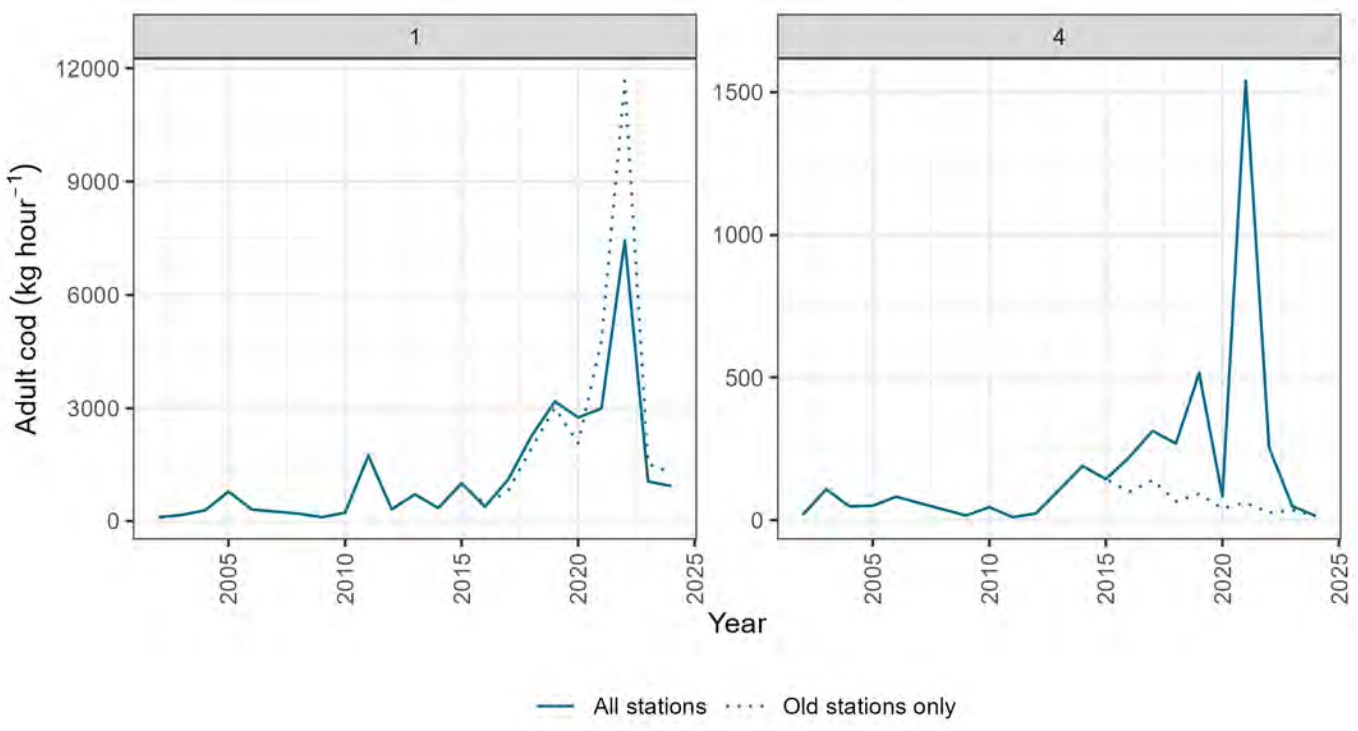

Figure S3: Average BPUE of adult cod in The Sound including either all stations (full line), or only old stations (dotted line), for Quarter 1 and Quarter 4.

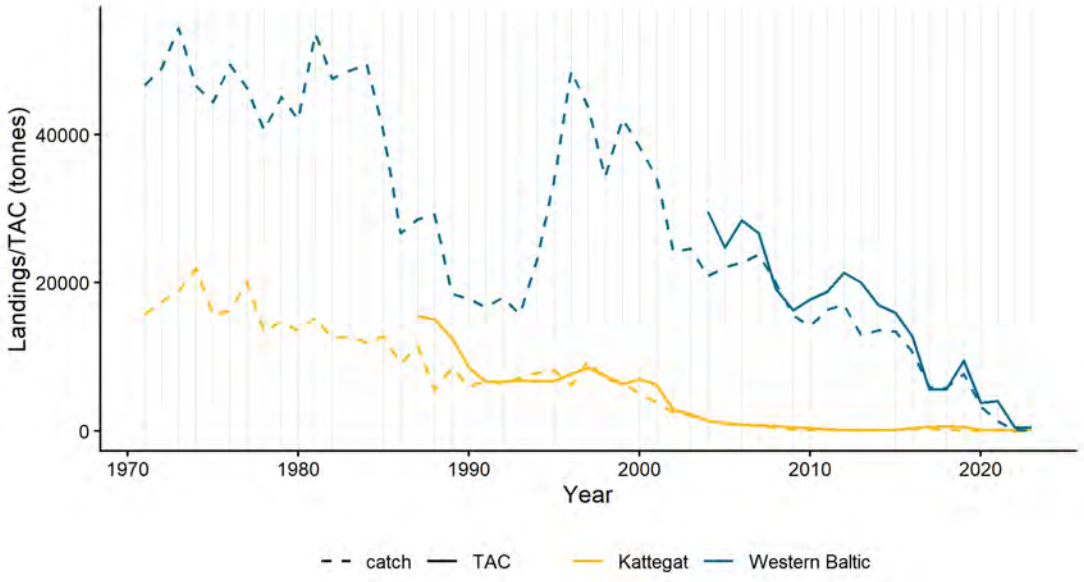

Figure S4: Reported landings for the Western Baltic cod stock (including The Sound, Arkona Sea and Belt Sea) and the Kattegat cod stock [23], together with corresponding total allowable catches (TACs) [24, 26].

	The Sound	Kattegat	Belt Sea	Arkona Sea
Quarter 1				
BPUE	23.9	**3.8**	**3.2**	**11.2**
juvenile	(12.2; 46.8)	**(2.4; 5.9)**	**(2.0; 5.3)**	**(7.9; 15.8)**
		p < 0.001	**p < 0.001**	**p = 0.02**
BPUE	1384.1	**23.8**	**63.0**	**161.4**
adults	(833.4; 2298.6)	**(16.8; 33.8)**	**(41.3; 96.1)**	**(129.4; 201.2)**
		p < 0.001	**p < 0.001**	**p < 0.001**
size	52.6	**41.8**	**43.5**	**42.0**
	(48.6; 57.0)	**(36.4; 47.8)**	**(38.7; 48.8)**	**(40.4; 43.7)**
		p = 0.002	**p = 0.004**	**p < 0.001**
Quarter 4				
BPUE	3.8	3.2	4.4	**12.7**
juvenile	(2.3; 6.2)	(2.2; 4.5)	(3.1; 6.1)	**(9.8; 16.3)**
		p = 0.5	p = 0.6	**p < 0.001**
BPUE	192.6	**10.0**	**12.2**	141.2
adults	(118.2; 313.7)	**(6.3; 16.0)**	**(7.8; 18.9)**	(118.8; 168.0)
		p < 0.001	**p < 0.001**	p = 0.2
size	56.0	**29.7**	**26.3**	**41.2**
	(51.8; 60.6)	**(25.2; 35.0)**	**(22.9; 30.1)**	**(39.7; 42.7)**
		p < 0.001	**p < 0.001**	**p < 0.001**

Table S8: Results from the generalised linear mixed models used to assess differences in the cod stock between The Sound and the other areas (Kattegat, Belt Sea and Arkona Sea) based on data from the Baltic International Trawl Survey. The table shows estimated values (including 95% confidence intervals) and p-values for the different areas for each response variable: BPUE (kg hour^{-1}) of juvenile ($\leq$ 25 cm) and adult (>25 cm) cod, as well as 95th percentile size (cm) of cod. Significant differences from The Sound (p <0.05) are indicated in bold. Results are shown separately for Quarter 1 and Quarter 4.

Species	**The Sound**	**Kattegat**
shore crab	5.7	**15**
	(3.9; 8.4)	**(9.6; 25)**
		p <0.001
black goby	0.014	0.036
	(0.0037; 0.051)	(0.0055; 0.23)
		p = 0.4
goldsinny wrasse	0.057	**1.0**
	(0.011; 0.29)	**(0.094; 11)**
		p = 0.04

Table S9: Shows the predicted CPUE of the different mesopredator species caught in fyke nets along the Swedish coast, with associated 95% confidence intervals and p-values for the difference between the two areas, Kattegat (SD 21) and The Sound (SD 23). Values marked in bold indicate a significant difference from The Sound (p <0.05).

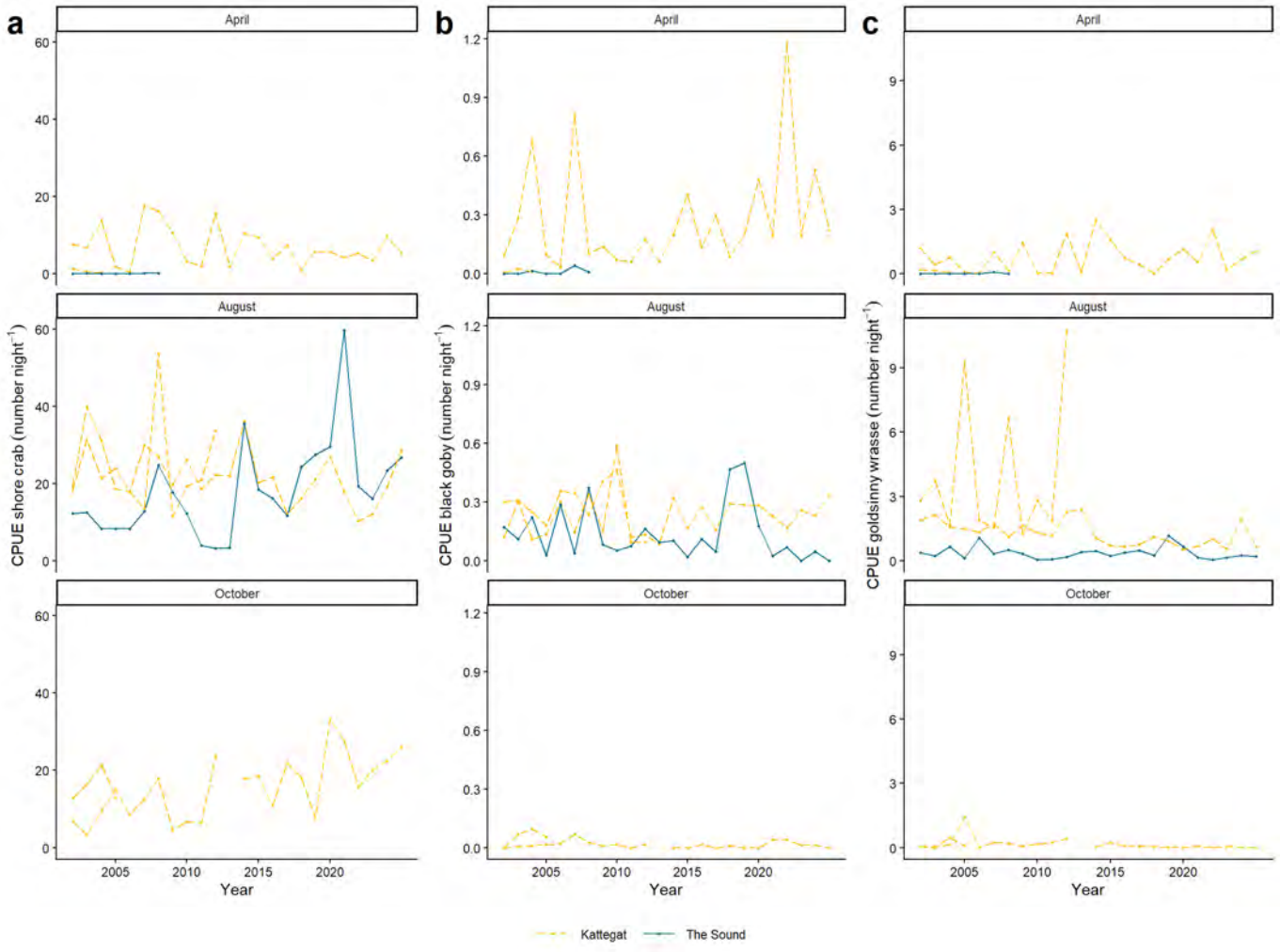

Figure S 5: Yearly average CPUE of (a) shore crab, (b) black goby and (c) goldsinny wrasse caught with fyke nets along the Swedish coast, in The Sound and the Kattegat, respectively. Data are presented for each sampling month separately due to seasonal patterns in habitat use and the effect of water temperature on activity. Note that the location of some of the fished stations changed in 2021 (see Table S6).

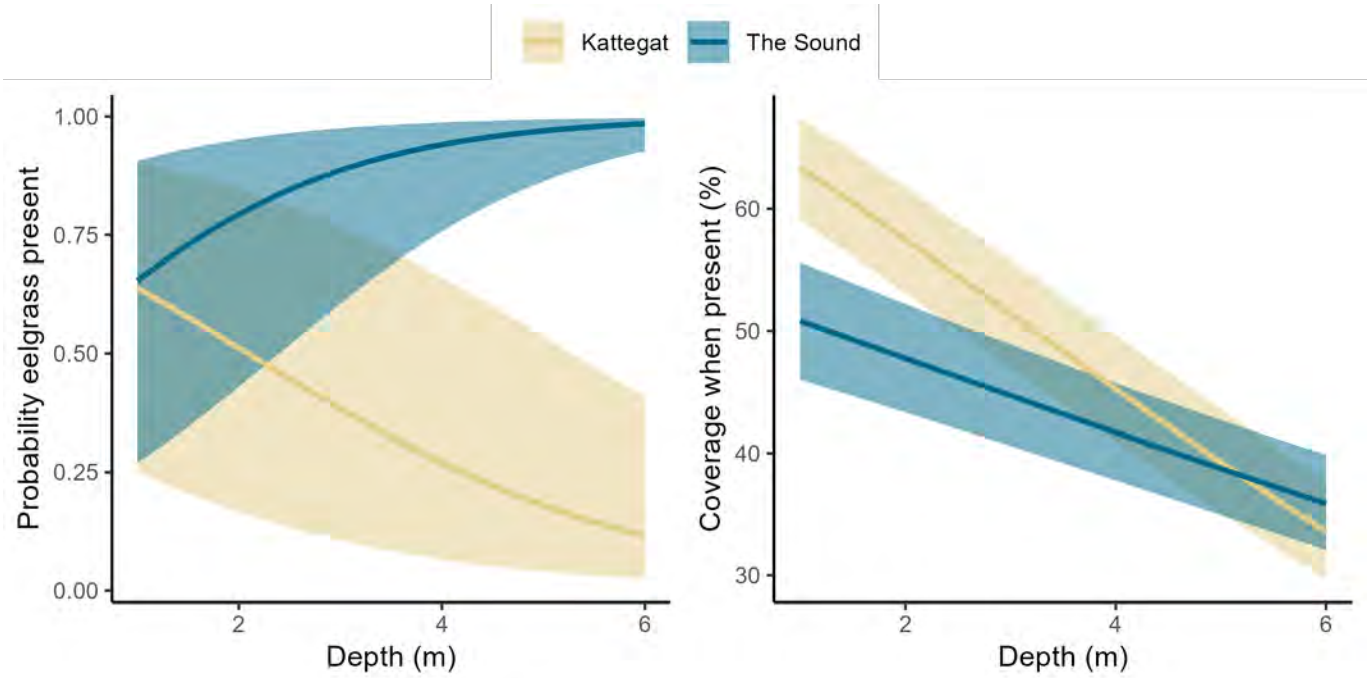

Figure S 6: SD-specific predicted effect of depth on probability of eelgrass being present and its coverage when present, based on the zero-inflated generalised linear mixed model descibed in the main text.

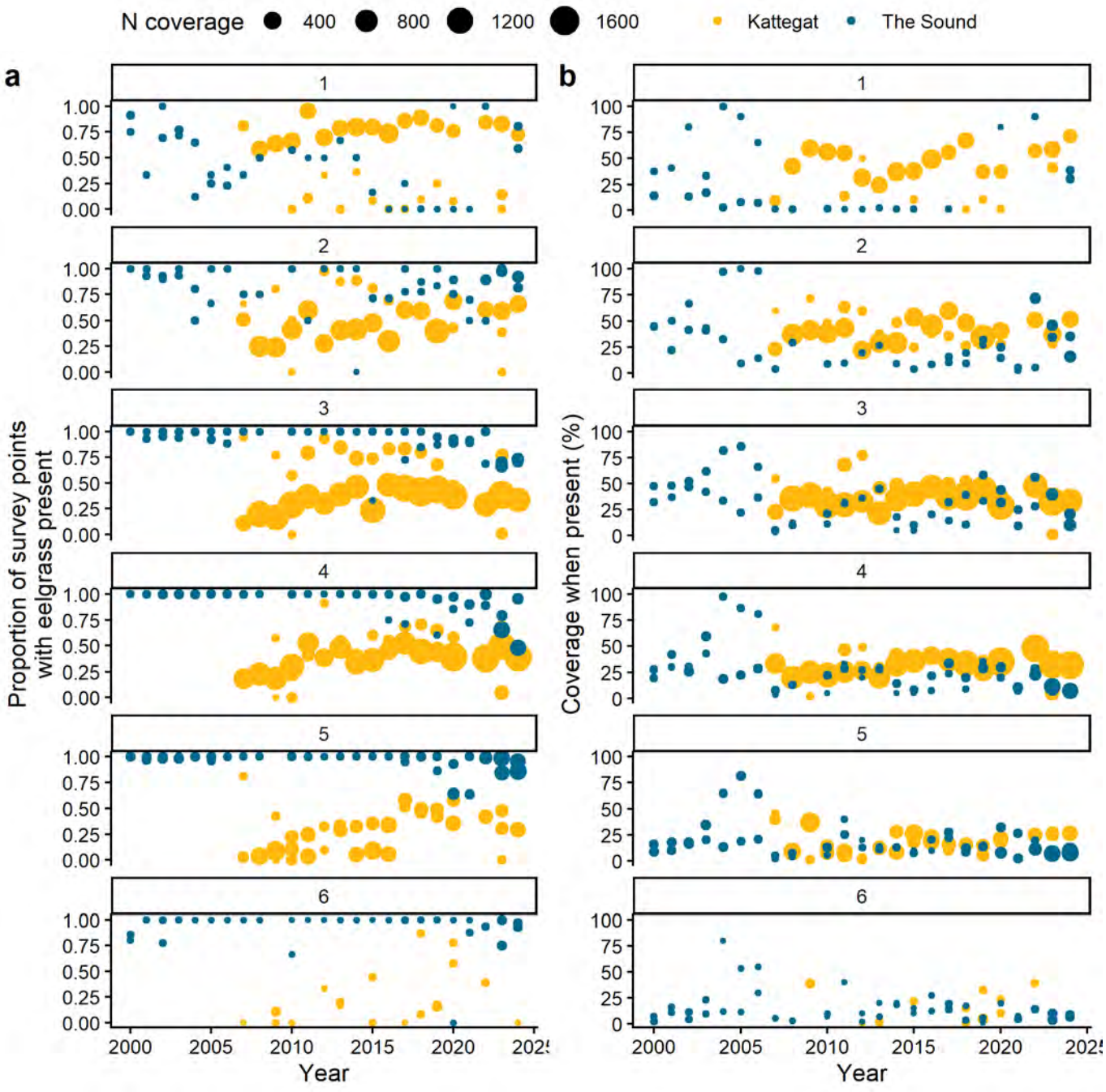

Figure S 7: Yearly averages of (a) proportion of survey points with eelgrass present and (b) eelgrass coverage in survey points when present, in The Sound and the Kattegat, respectively, for each depth.

3.2 Modelling results: trophic level abundances, dynamics, and cod extinction times

3.2.1 Two-parameter phase diagrams and dynamics

The impact of natural mortality of cod on all trophic levels is displayed in Figure S8. Here, the mean abundances are shown in the parameter space (ν_{C_2}, ν_{C_1}). As expected, the mean abundances for cod decrease with increasing cod natural mortalities. The decrease of the cod populations, as we will show below, is not linear. Cod populations experience a slow decrease at low natural mortality and then an acceleration when the natural mortality of adult cod is increased. The first two panels in Figure S8(a) display this decrease in cod populations, which remain very similar for both juvenile and adult cod. We have overlapped in these diagrams those values of natural mortality estimated from the Western Baltic stock (blue line, see Table S2). These levels of natural mortality allow for stable cod populations but are found close to the extinction boundary, meaning that other pressure on cod e.g., increased fishing, could increase the risk of collapse. The increase of cod natural mortality has a profound impact on the other trophic levels. For instance, at low cod mortality, both cod and eelgrass are very abundant. This is also associated with depleted or very low mesopredator abundances. When the cod populations collapse, the mesopredators display the largest abundances, coexisting with mesoherbivores, smaller areas of eelgrass and very large densities of algae. A slight decrease in the cod population allows the coexistence of all the trophic levels with deterministic fluctuations. This observation will be discussed below by means of the presence-abundance indices.

Figure S9 shows the dynamics of each trophic level for different values of cod natural mortality. For all the parameter values, the abundances show self-sustained fluctuations in time, typical for predator-prey systems. Panel (a) displays a scenario in which cod populations are very large due to very low natural mortality. Here, the abundance of both adult and juvenile cod increase over the years, while abundances of mesopredators decrease until collapse. The increase of cod populations causes an oscillatory increase in eelgrass until they stabilise at the maximum carrying capacity. The oscillatory regime for eelgrass is accompanied by strong fluctuations of algae, which collapse after about 30 years, with the subsequent collapse of mesoherbivores, which depend on the filamentous algae for food. Here, very large cod populations thus destabilise the trophic levels. Despite the collapse of mesopredators, cod populations can still persist probably due to the food income provided by herring. Panels (b) to (e) show results for higher natural mortality for cod populations, which allow for coexistence between all the trophic levels, despite the cod populations showing a decreasing tendency. All these analyses also reveal self-sustained ocillations, which can be very large, with filamentous algae and mesoherbivores reaching very low population values before recovering again. When the natural mortality for cod exceeds critical thresholds, cod populations rapidly collapse and the other trophic levels keep fluctuating [see panel (f)].

The impact of perturbations on eelgrass in the abundances of the trophic levels is shown in Figures S10 and S11. First, we investigate the impact of decreasing the available habitat for eelgrass (ω_E) and increasing the eelgrass destruction rate (η_E), considering the natural mortality for juvenile and adult cod estimated from the Western Baltic stock ($\nu_{C1} = 0.598$ and $\nu_{C1} = 0.201$). The results, displayed in Figure S10, reveal that the amount of cod is extremely low, and the abundances of both adult and juvenile cod decrease when the destruction rate of eelgrass increases and when the available habitat for eelgrass is reduced. Under this scenario, all trophic levels can coexist, except for eelgrass, which, as expected, disappears when its destruction rate is very large and when no habitat is available. Increasing the perturbations on eelgrass also involves a decrease in the densities of mesopredators and filamentous algae. Here, the extremely low cod population cannot exert top-down control on mesopredators.

The same analyses have been repeated considering lower natural mortality for cod, with $\nu_{C1} = 0.25$ (juvenile) and $\nu_{C2} = 0.2$ (adult), see Figure S11. Similarly to the previous analyses, the abundance of eelgrass decreases with increasing η_E and decreasing ω_E. However, the mean abundances for eelgrass

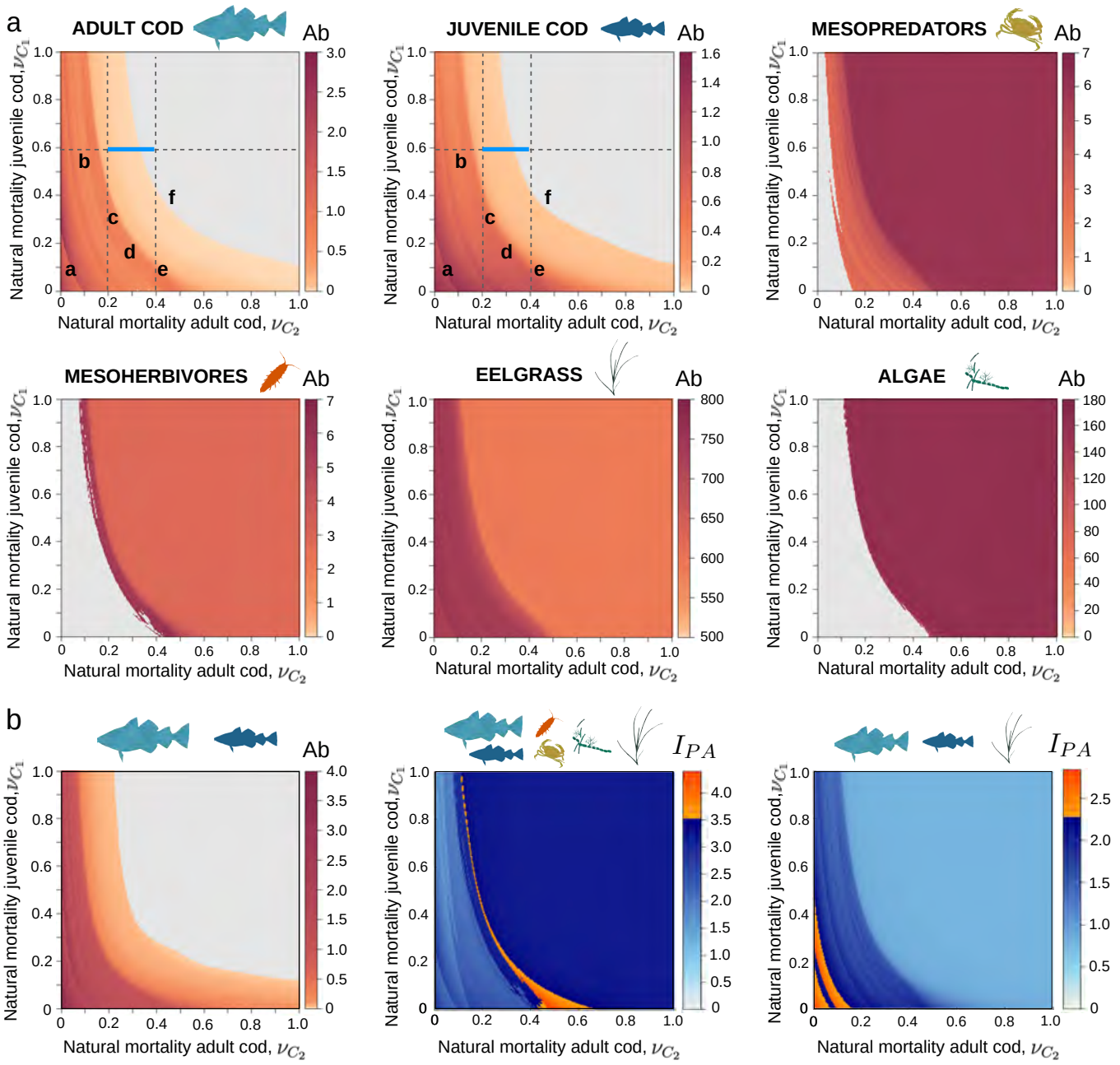

Figure S8: **Abundance diagrams and presence-abundance indices at varying levels of cod natural mortality without fishing**. (a) Mean population abundances varying levels of natural mortality for both juvenile and adult cod populations [parameter space (ν_{C2}, ν_{C1})] are computed by averaging the populations over 75-year simulations. Abundances are given in tonnes km^{-2} for all trophic levels, except for eelgrass, which is given in area (km^2). The populations ending up in collapses before 75 years are set to zero. Here we consider no cod fishing and no perturbations on eelgrass, i.e., $\eta_{C_2} = 0$, $\omega_E = 1$ and $\eta_E = 0$. The values for all the other parameters are provided in Table S2. The inner blue lines in the diagrams for juvenile and adult cod show the mortality estimated for the Western Baltic cod stock (Table S2). The dynamics for the parameter values indicated with the letters are shown in Figure S9 for all the variables. (b) The first panel shows the total abundance of cod (juveniles + adults). The presence-abundance indices, $I_{PA}(n)$, have been computed from the diagrams shown in (a), considering all trophic levels (second panel, with $n = 6$) and the cod plus eelgrass (third panel, with $n = 3$). The maximum and minimum values are: $I_{PA}^{max}(6) = 4.40$ and $I_{PA}^{min}(6) = 0.88$; $I_{PA}^{max}(3) = 2.84$ and $I_{PA}^{min}(3) = 0.78$. For the sake of visualisation, the values of the index are shown with a blue gradient together with an orange gradient for the 20% of the highest values.

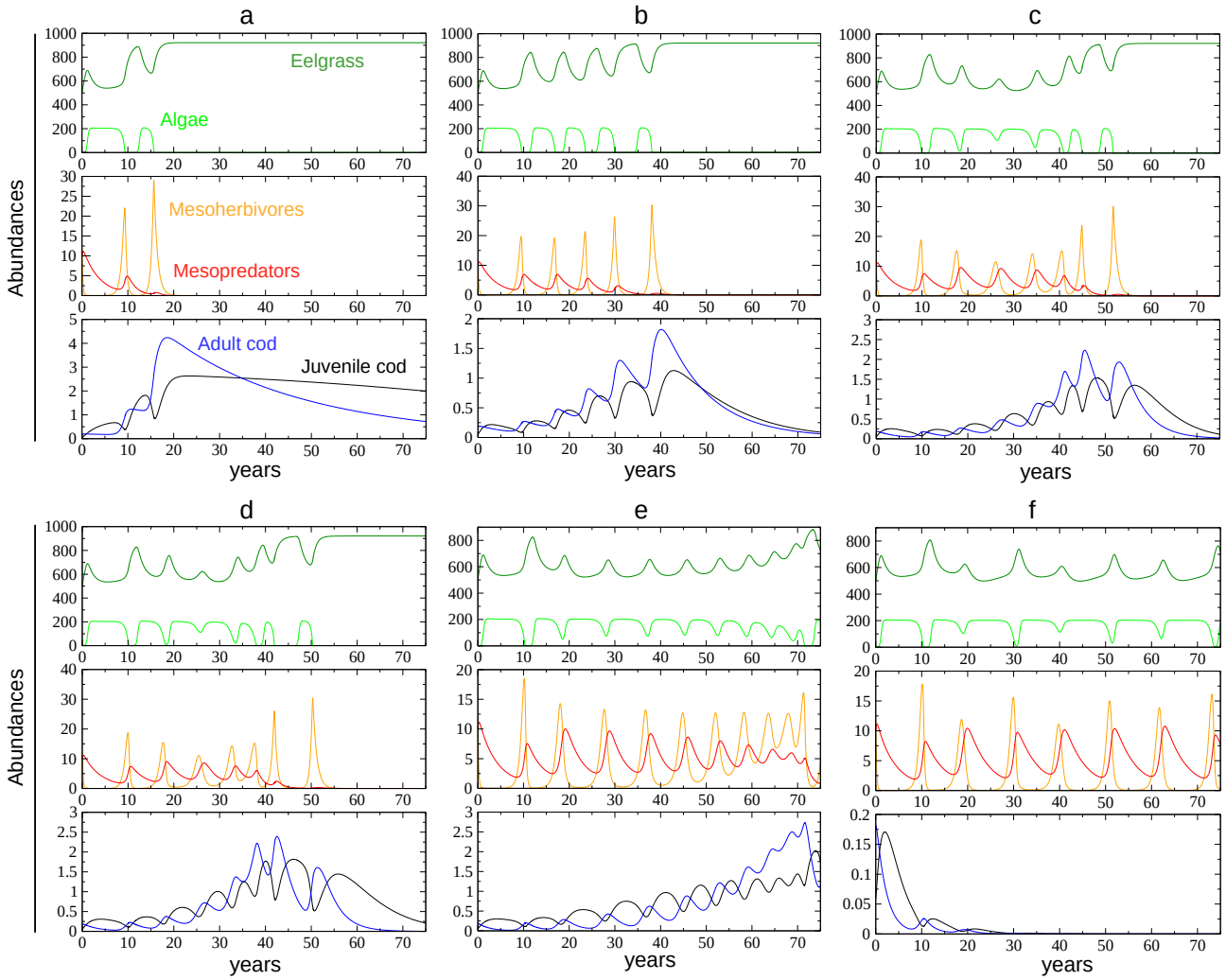

Figure S9: **Dynamics of each trophic level for different adult (ν_{C2}) and juvenile (ν_{C1}) cod natural mortality**. Each panel triplet illustrates the dynamics of all trophic levels under different natural mortality rates of cod, corresponding to the lettered scenarios in Figure S8: (a) $\nu_{C2} = 0.03$ and $\nu_{C1} = 0.08$; (b) $\nu_{C2} = 0.1$ and $\nu_{C1} = 0.54$; (c) $\nu_{C2} = 0.22$ and $\nu_{C1} = 0.3$; (d) $\nu_{C2} = 0.3$ and $\nu_{C1} = 0.14$; (e) $\nu_{C2} = 0.42$ and $\nu_{C1} = 0.08$; (f) $\nu_{C2} = 0.46$ and $\nu_{C1} = 0.4$.

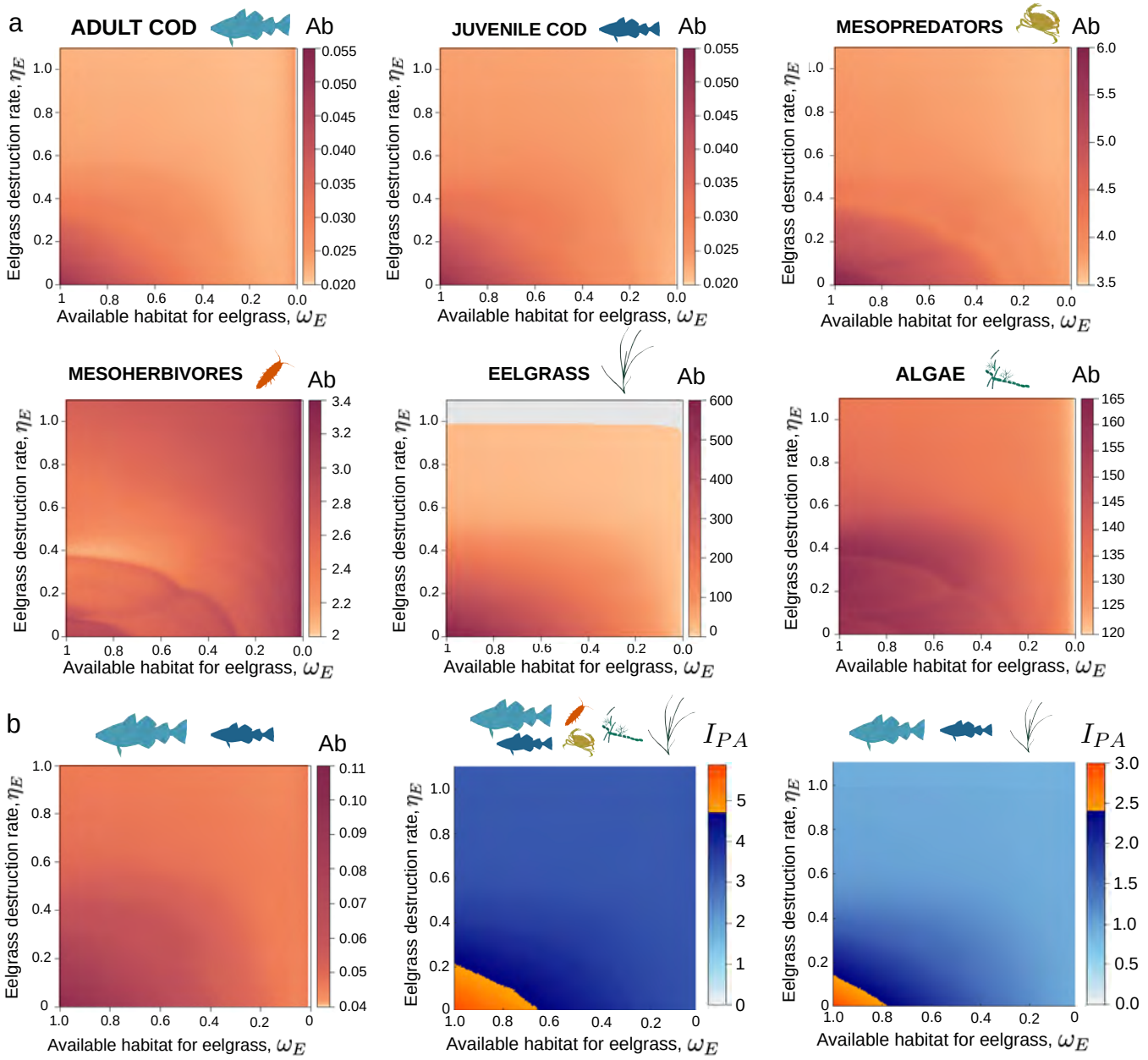

Figure S 10: **Abundance diagrams and presence-abundance indices at varying levels of perturbations on eelgrass**. (a) Abundance diagrams, computed with the cod natural mortality estimated from the Western Baltic stock, with $\nu_{C1} = 0.598$ and $\nu_{C2} = 0.201$, without including cod fishing. The values of the other parameters are provided in Table S2. (b) The first panel shows the total abundance of cod (juveniles + adults). The presence-abundance indices, $I_{PA}(n)$, have been computed from the diagrams shown in (a), considering all trophic levels (second panel, with $n = 6$) and the cod plus eelgrass (third panel, with $n = 3$). The maximum and minimum values are: $I_{PA}^{max}(6) = 5.89$ and $I_{PA}^{min}(6) = 3.13$; $I_{PA}^{max}(3) = 3$ and $I_{PA}^{min}(3) = 0.84$.

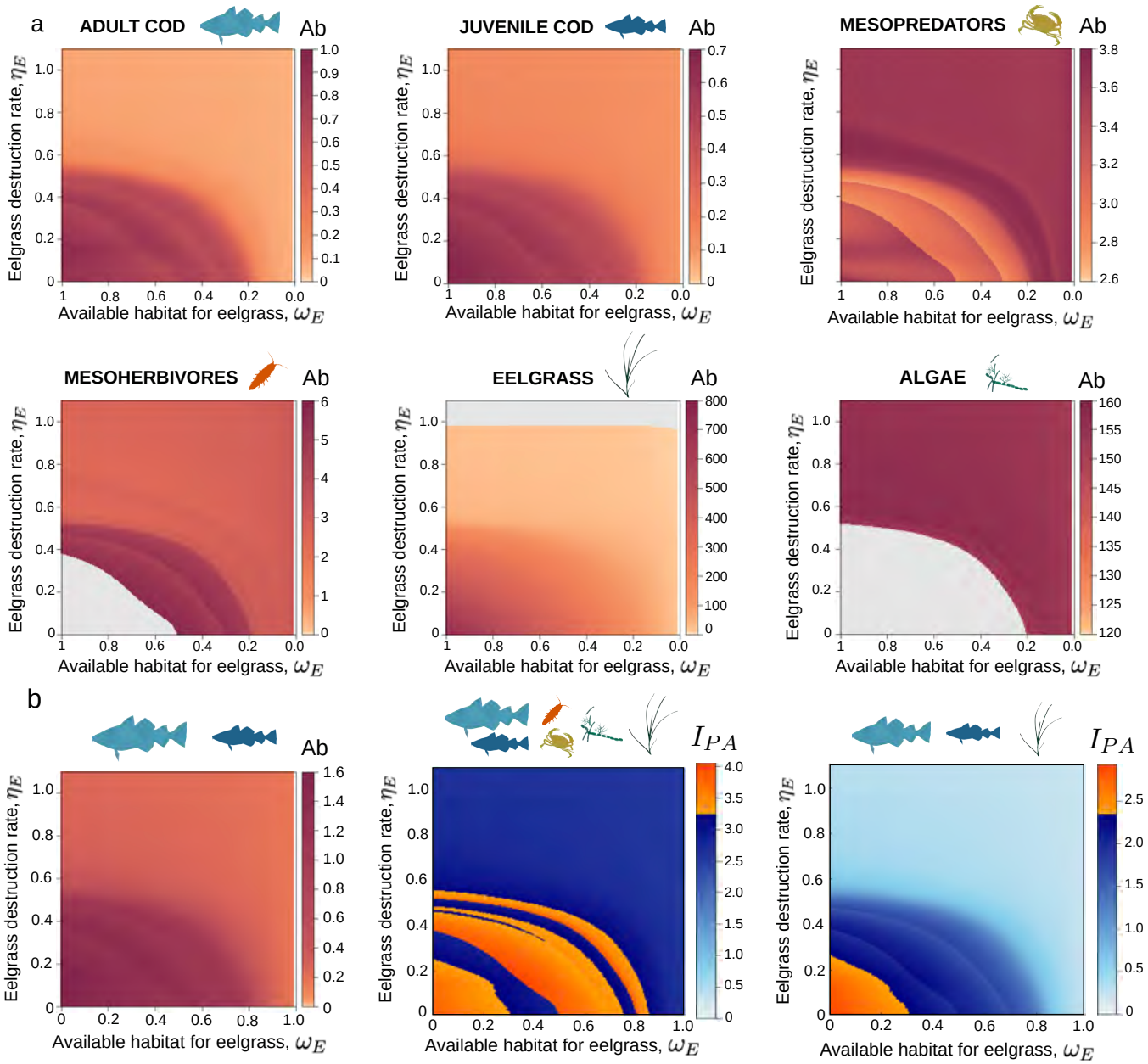

Figure S 11: **Abundance diagrams and presence-abundance indices at varying levels of perturbations on eelgrass with no cod fishing**. Same as in the Figure S10, here using lower cod mortality rates, i.e., $\nu_{C1} = 0.25$ and $\nu_{C2} = 0.2$, also with no cod fishing. The maximum and minimum values of the presence-abundance indices are: $I_{PA}^{max}(6) = 4.05$ and $I_{PA}^{min}(6) = 2.57$; $I_{PA}^{max}(3) = 2.93$ and $I_{PA}^{min}(3) = 0.21$.

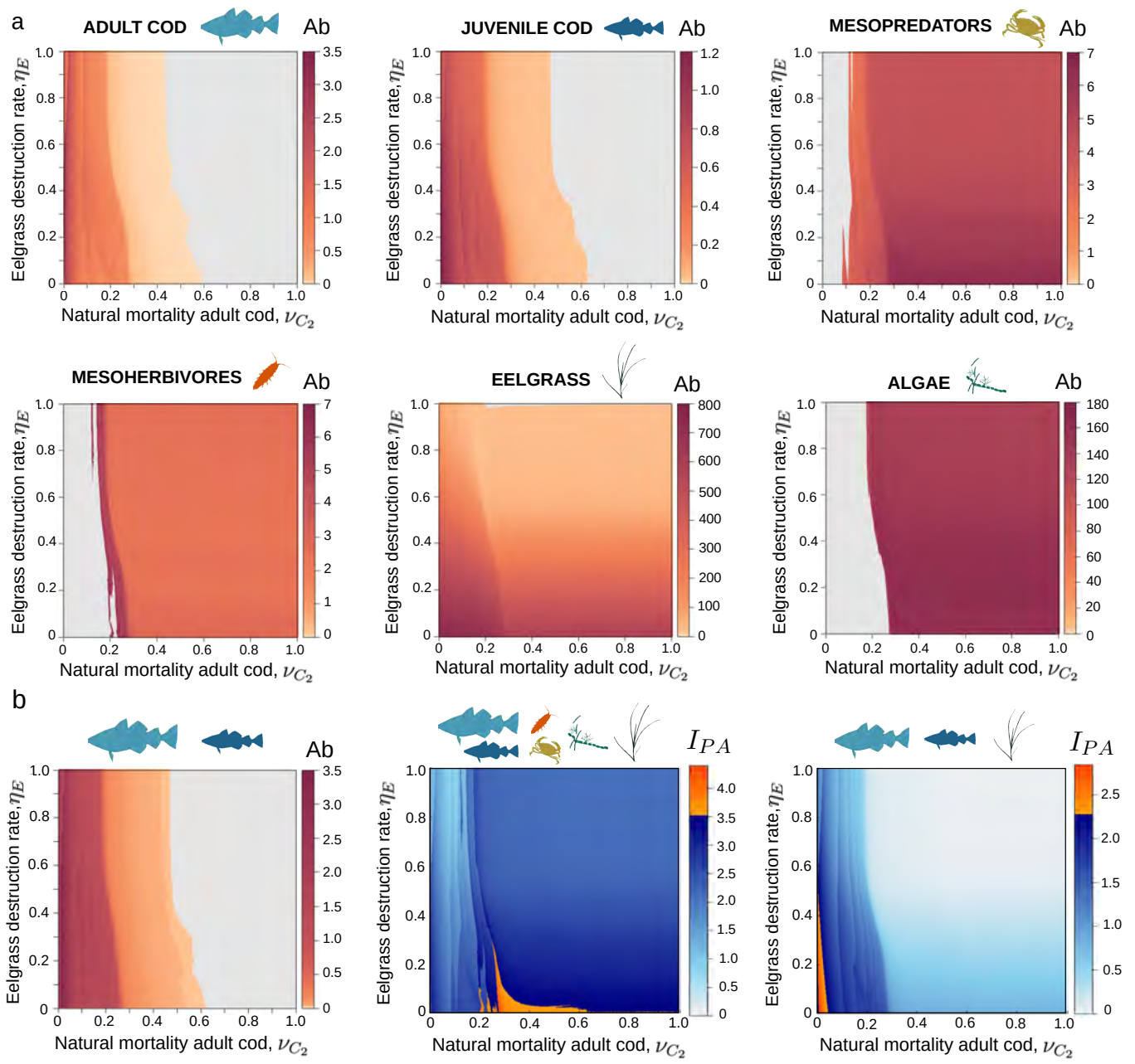

Figure S 12: **Abundance diagrams and presence-abundance indices at varying levels of adult cod natural mortality and perturbations on eelgrass with no cod fishing**. The abundances are now computed in the parameter space (ν_{C2}, η_E). Here we have set available area for eelgrass to $\omega_E = 1$ and the natural mortality of juvenile cod has been set to $\nu_{C1} = 0.25$, also without cod fishing $\eta_{C_2} = 0$. The values of the other parameters are provided in Table S2. $I_{PA}^{max}(6) = 3.94$ and $I_{PA}^{min}(6) = 0.65$; $I_{PA}^{max}(3) = 2.81$ and $I_{PA}^{min}(3) = 0$.

remain higher than in the previous figure, where the natural mortality for cod was larger. The positive effect of eelgrass on cod populations can be clearly seen. Those regions in the parameter space (ω_E, η_E) with larger abundance of eelgrass, i.e., low η_E and high ω_E, are those showing larger cod populations. These abundances for cod are about 1.8-fold larger as compared to the results obtained using the natural mortality from the Western Baltic stock. Here, as expected, larger amounts of eelgrass involve larger cod populations and thus a decrease in mesopredator populations and larger abundance of mesoherbivores.

Next, we have computed the mean abundances of the trophic levels by combining an increase in the adult cod natural mortality η_{C2} and an increase in the rate of eelgrass destruction η_E, using $\omega_E = 1$ and without considering cod fishing (see Figure S12). Generally, an increase in the eelgrass destruction rate makes the population of cod more sensitive to increases in natural mortality. For instance, with tiny perturbations on eelgrass, i.e., $\eta_E \to 0$, the adult cod mortality that results in the largest abundances (≈ 0.5 to 3.5 tonnes km^{-2}) is about $\nu_{C2} \approx 0.3$, but when the destruction rate of eelgrass increases, the natural mortality of adult cod allowing for this largest abundances decreases to $\nu_{C2} \approx 0.2$, meaning that the population of cod (both juveniles and adults) are more fragile. As expected, an increase of η_E decreases the abundance of eelgrass. This decrease is very large when increasing adult cod mortality. For instance, for $\eta_E, \nu_{C2} \approx 0$ the abundance of eelgrass is close to the carrying capacity (987 km^2), having an area of $\sim$ 800 km^2. The combination of large natural mortality for adult cod and intermediate destruction rate of eelgrass (e.g., $\eta_E = 0.5$) can cause an eightfold reduction of the eelgrass area.

The same analyses have been carried out including adult cod fishing ($\eta_{C_2} = 0.2$), and a 30% reduction of the available habitat for eelgrass, i.e., $\omega_E = 0.7$. The results, shown in Figure S13, show a drastic reduction of the cod population in the parameter space (ν_{C_2}, η_E). The mortality of adult cod involving the collapse of the cod populations (considering both juvenile and adult) is lower for $\eta_E \to 1$, i.e., $\nu_{C_2} \approx 0.35$ (without fishing and $\omega_E = 1$ it was $\nu_{C_2} \approx 0.6$, cf. Figure S12). As the destruction rate of eelgrass increases, this value is $\nu_{C_2} \approx 0.25$. The same results for the previous figure without simulating cod fishing and with $\omega_E = 1$ were $\nu_{C_2} \approx 0.47$. Moreover, the abundance of the cod population suffers a four-fold decrease for adult cod and a twofold decrease for juvenile cod (cf. cod abundances in Figure S12.)

3.2.2 Presence-abundance indices

In this section we apply the presence-abundance index (I_{PA}) defined in Section 2.3. This index, which allows us to identify those parametric regions where the presence and abundance of trophic levels are maximised, can be computed considering n different trophic levels, and its values range from 0 to n. Hence, an index $I_{PA} = n$ means that all trophic levels are found and have maximum abundance values in a given parametric domain. We compute this index for all trophic levels together $n = 6$, and for cod plus eelgrass $n = 3$. Specifically, we provide measures of the maximum, $I_{PA}^{max}(n)$; and minimum $I_{PA}^{min}(n)$ values. This simple index allows us to identify those values of parameters maximising the presence and abundance of the trophic levels as well as to identify ecological scenarios with high ecosystem services (i.e., large cod and eelgrass abundance). One of our goals is to explore how these indices change upon parameter changes.

First, we computed the index from the abundance diagrams displayed in Figure S8, where the mean abundances were computed at varying levels of natural cod mortality and no disturbances on eelgrass, i.e., no eelgrass destruction and full available habitat for eelgrass. In agreement with the previous results on two- and one-dimensional abundance diagrams, the scenarios where all the trophic levels coexist with maximum abundances ($I_{PA}^{max}(6) = 4.40$) are found for cod mortality around $\nu_{C_1} \in [0, 0.1]$ and $\nu_{C_2} \in [0.4, 0.6]$. While the maximum index values for cod and eelgrass are found for very low values of cod mortality ($I_{PA}^{max}(3) = 2.84$), the index for the whole system is maximised when cod populations are not at their maximum. Under this scenario with very large cod populations, the

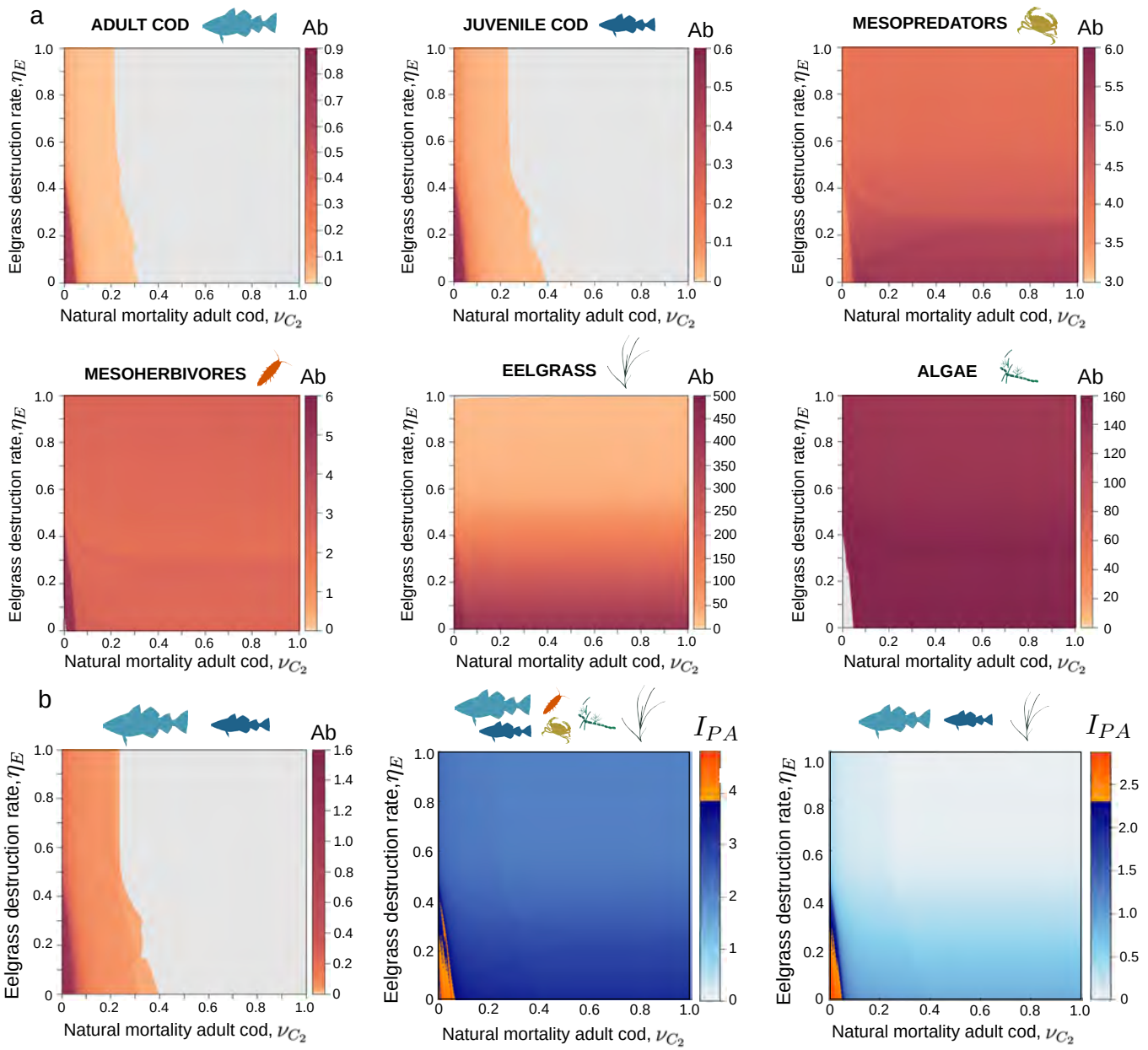

Figure S 13: **Abundance diagrams varying levels of adult cod mortality and eelgrass destruction rate with cod fishing and a reduction of available eelgrass habitat**. Same as in Figure S12 with $\nu_1 = 0.25$, fishing mortality of adult cod $\eta_{C_2} = 0.2$, with $\eta_{C1} = \eta_{C2}/12.807$ [23], and a 30% of reduction of the available eelgrass habitat i.e., $\omega_E = 0.7$. Here, the maximum and minimum values of the indices are: $I_{PA}^{max}(6) = 4.80$ and $I_{PA}^{min}(6) = 1.98$; $I_{PA}^{max}(3) = 2.88$ and $I_{PA}^{min}(3) = 0$.

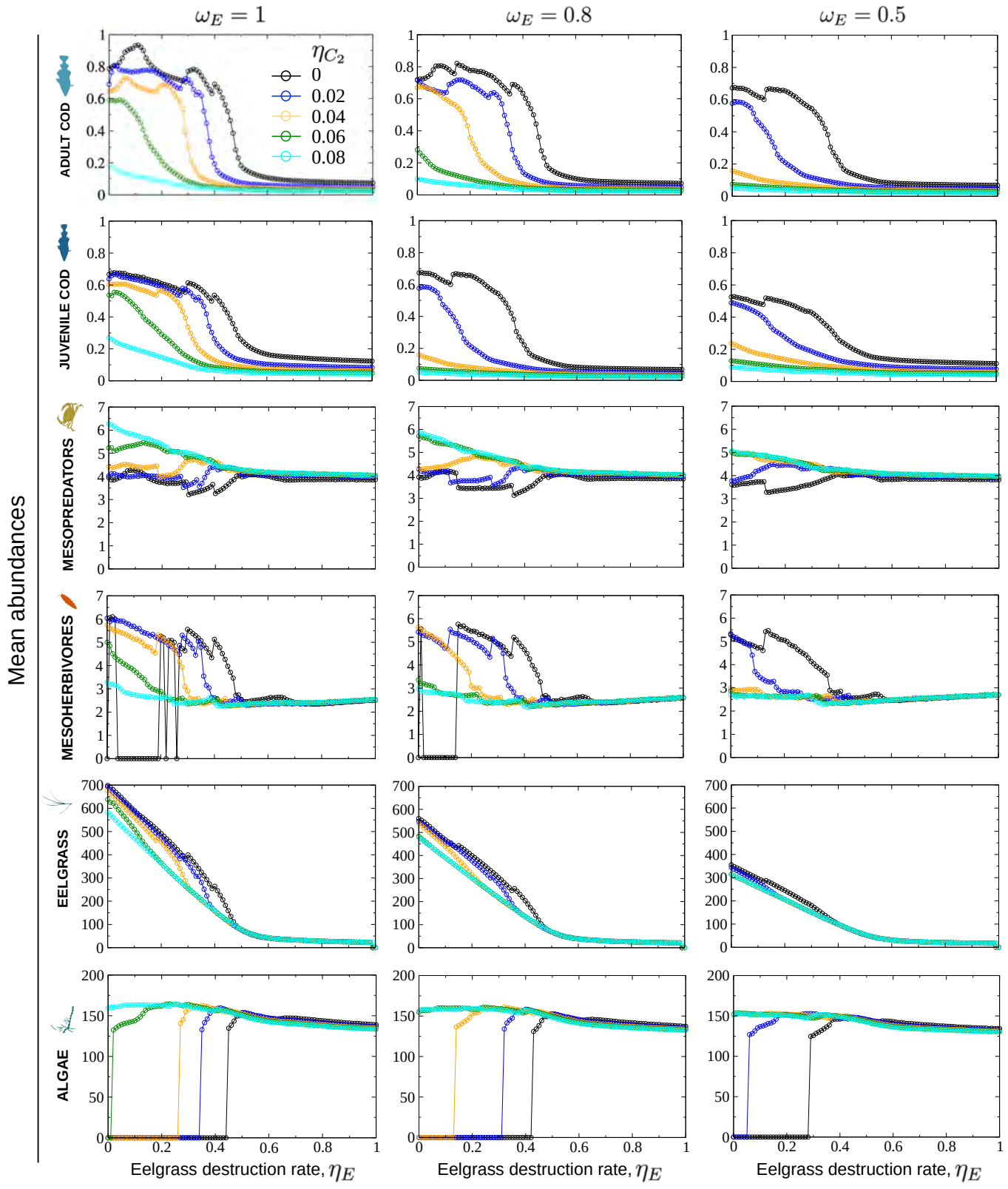

Figure S14: Changes in the mean abundances over 75 years with increasing eelgrass destruction rates for three different fractions of available eelgrass habitat (ω_E in the columns). Here we set $\nu_{C_1} = 0.24$ and $\nu_{C_2} = 0.22$. In each panel we display the abundances at varying levels of the fishing mortality of adult cod, with : $\eta_{C_2} = 0$ (black); $\eta_{C_2} = 0.02$ (blue); $\eta_{C_2} = 0.04$ (orange); $\eta_{C_2} = 0.06$ (green); $\eta_{C_2} = 0.08$ (cyan). The values of the other parameters are provided in Table S2.

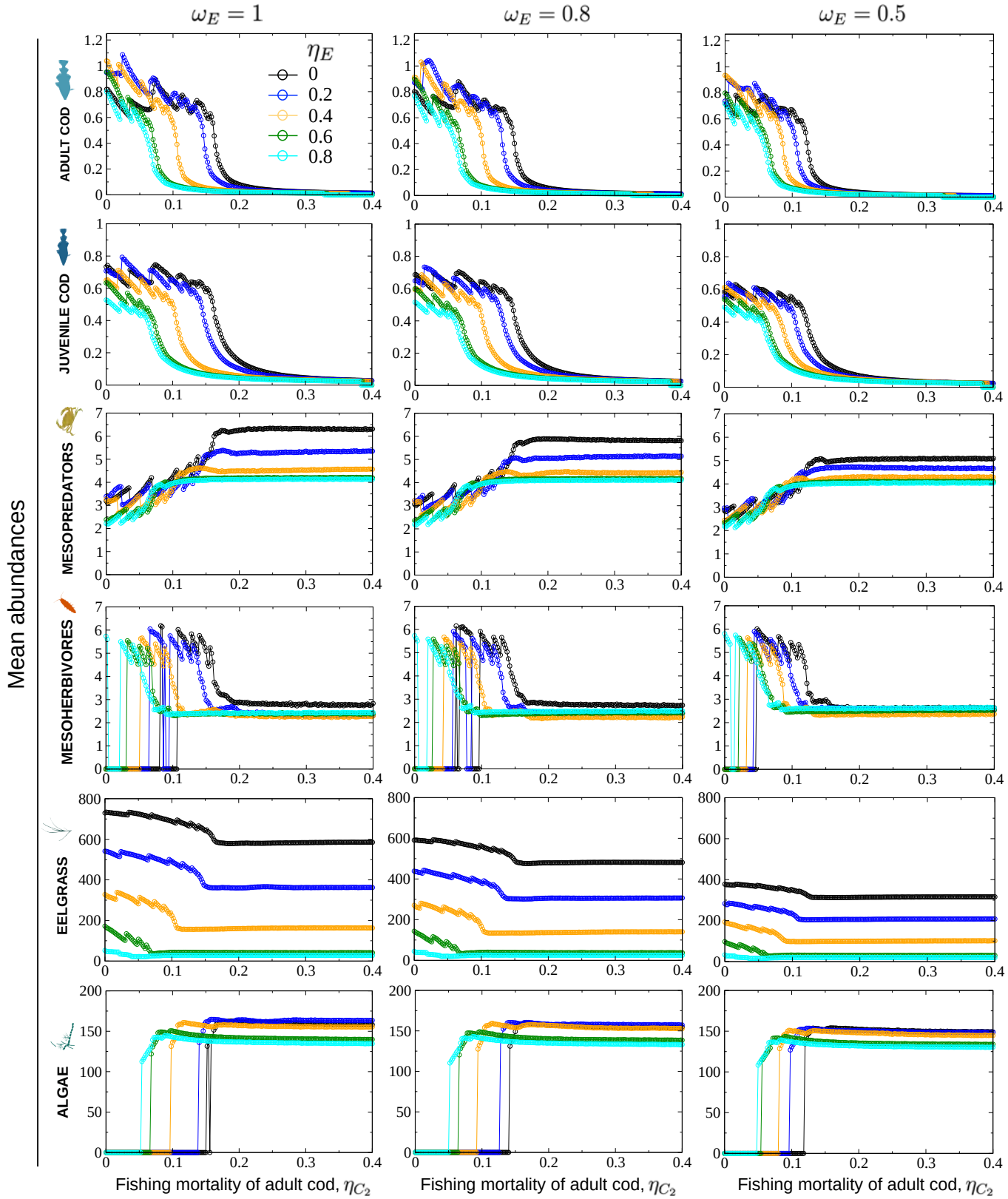

Figure S15: Changes in the mean populations over 75 years with increasing levels of fishing mortality of adult cod for three different fractions of available eelgrass habitat (ω_E in the columns). Here we set $\nu_{C_1} = 0.15$ and $\nu_{C_2} = 0.2$. In each panel we display the abundances at varying levels of eelgrass destruction rates, with : $\eta_E = 0$ (black); $\eta_E = 0.2$ (blue); $\eta_E = 0.4$ (orange); $\eta_E = 0.6$ (green); $\eta_E = 0.8$ (cyan). The values of the other parameters are provided in Table S2.

index value is at its minimum i.e., $I_{PA}^{min}(6) = 0.88$. The minimum value of the index applied to cod and eelgrass, with $I_{PA}^{min}(3) = 0.78$ is found when the mortality of cod is very high.

The perturbations on eelgrass has a large effect on these indices (see Figure S10). For instance, using the values of cod natural mortality estimated from the Western Baltic, the maximum and minimum values of this index are given by: $I_{PA}^{max}(6) = 5.89$ and $I_{PA}^{min}(6) = 3.13$; $I_{PA}^{max}(3) = 3$ and $I_{PA}^{min}(3) = 0.84$. The maximum values of the index are found when the destruction rate of eelgrass is very close to zero and the available habitat for eelgrass is at its maximum. Changes in these two parameters i.e., increasing η_E and decreasing ω_E, rapidly decrease this index. This effect is more dramatic for the index applied to cod plus eelgrass only, where the maximum value restricted to a very small region of the parameter space.

When instead decreasing cod natural mortality ($\nu_{C_1} = 0.25$ and $\nu_{C_2} = 0.2$), shown in Figure S11, we get $I_{PA}^{max}(6) = 4.05$ and $I_{PA}^{min}(6) = 2.57$; $I_{PA}^{max}(3) = 2.93$ and $I_{PA}^{min}(3) = 0.21$. The maximum values of the indices applied to the entire system and to eelgrass plus cod are also found in the bottom-left corner of the parameter space (ω_e, η_E), with a very sharp decrease (i.e., 10-fold reduction) for the eelgrass-cod values with increasing levels of destruction of eelgrass.

The indices computed over the parameter space (ν_{C_2}, η_E) displayed in Figure S12, where no cod fishing is considered and with $\omega_E = 1$, are: $I_{PA}^{max}(6) = 3.94$ and $I_{PA}^{min}(6) = 0.65$; $I_{PA}^{max}(3) = 2.81$ and $I_{PA}^{min}(3) = 0$. Here, again, the maximum values for the entire system are found when the destruction rate of eelgrass is close to zero and adult cod natural mortality are around $\nu_{C_2} \in [0.3, 0.6]$. It means that the entire system remains stable for the simulated years if the population of cod is not very large. The index for eelgrass plus cod remains at a maximum also for very small values of ν_{C_2}, and the destruction of eelgrass decreases this maximum value.

Finally, we also computed the indices in the parameter (ν_{C_2}, η_E), now including a fishing mortality of $\eta_{C_2} = 0.2$ and reducing the available habitat for eelgrass a 30%. This scenario involves $I_{PA}^{max}(6) = 4.80$ and $I_{PA}^{min}(6) = 1.98$; $I_{PA}^{max}(3) = 2.88$ and $I_{PA}^{min}(3) = 0$. Here, although the maximum values of the index remain similar to those without cod fishing and with a full available habitat for eelgrass, the combinations of parameters giving these maximum values is greatly decreased. That is, for very small increases in the natural mortality of adult cod or eelgrass destruction, the indices dramatically decrease (see Figure 13).

3.2.3 One-parameter phase diagrams

In order to extend the results on two-parametric phase diagrams and to better visualise how the abundances change when tuning key parameters related to cod mortality and eelgrass destruction, we have built one-dimensional abundance diagrams. To do so, we first compute the mean abundances as in the previous section at varying levels of eelgrass destruction rates, η_E. The results are shown in Figure S14 for different fractions of available habitat for eelgrass (ω_E, in the columns of Figure S14) and for increasing values of cod fishing mortality (different colours in the panels of Figure S14), using $\nu_{C_1} = 0.24$ and $\nu_{C_2} = 0.22$. The abundance of eelgrass, which decreases linearly with η_E, clearly diminishes when its available habitat is reduced. These abundances are also affected by increasing cod fishing mortality, which produce a further decrease of the area populated by eelgrass. While the abundance of eelgrass decreases linearly as its rate of destruction increases, the cod population does not decrease linearly. At low levels of cod fishing, cod populations remain at similar levels. However, a small increase in fishing mortality causes a marked decline (see the first two rows in Figure S14). This means that although cod abundance may appear stable under increased fishing mortality, it could collapse very rapidly. The simulations carried out for smaller values of the available habitat for eelgrass further show the key role of eelgrass in favouring cod populations. For instance, with $\omega_E = 1$, i.e., full habitat availability, the populations of cod keep high abundances with small η_E and for fishing mortality up to 0.04. However, when the available habitat for eelgrass is reduced by half, a small increase in the cod fishing mortality drives the population of cod towards collapse.

Figure S14 also shows that cod control of mesopredator abundance is highly sensitive to cod fishing mortality. Without fishing or with very low fishing mortality, mesopredator populations are smaller compared to scenarios with higher levels of cod fishing mortality. Lower mesopredator abundance correlates with higher mesoherbivore abundance and, therefore, with very low or no filamentous algae. Interestingly, both the destruction of eelgrass and the increase in the cod fishing mortality promote very large abundance of filamentous algae. This scenario is particularly evident when the fraction of available habitat for eelgrass is decreased, giving place to abundant algae. Finally, we want to note that the transition from no algae to higher densities of algae as eelgrass destruction rates increase is very sharp, as the lower panels in Figure S14 show.

Second, we also compute one-dimensional abundance diagrams at varying levels of cod fishing mortality. The results are shown in Figure S15. Here, the decrease in the abundance of eelgrass is not linear. When fishing mortality is small, large cod abundances are found together with depleted mesopredator abundances and large mesoherbivore populations. This is translated into absent or low densities of filamentous algae and wider areas occupied by eelgrass. This pattern is clearly affected by the eelgrass destruction rates. When eelgrass destruction rate is high, cod populations decrease substantially, favouring an increase in mesopredators with the corresponding decrease of mesoherbivores and the increase of algae, which coexist with reduced eelgrass areas. It is worth noting that filamentous algae can rapidly increase with increasing cod fishing mortality, as we observed with increasing the destruction rate of eelgrass.

3.2.4 Impact of increasing eelgrass destruction and adult cod fishing mortality on cod and eelgrass

As described in the main manuscript, a continuous increase in the eelgrass destruction rate (η_E) involves a linear decrease of the mean eelgrass abundance. However, such an increase in η_E causes a nonlinear decrease of the population of cod: for very low and increasing values of η_E, the population of cod remain more or less constant. However, at larger and increasing eelgrass destruction rates the population of cod rapidly goes down. The relationship between the eelgrass destruction rate and mean cod abundance is well fitted by an inverted sigmoidal function. Specifically, a four-parameter logistic model provides a very good fit. This model results in

$$\bar{C}_{1,2}(\eta_E) = A + \frac{L - A}{1 + \exp(k\,(\eta_E - \eta_{E_0}))}. \tag{3.1}$$

The explanation of the parameters of this function and the fitting procedure are provided in the Section 2.4. Figure 6 in the main manuscript displays the best fit performed with this logistic model (with coefficient of determination $R^2 = 0.992$), obtaining $A = 0.3108$, $L = 1.5336$, $k = 12.57$, and $\eta_{E_0} = 0.5613$.

The analysis of how cod fishing impacts on both eelgrass and cod populations is shown in Figure 6(b) in the main manuscript. First, the decrease of the population of cod at increasing η_{C_2} follows a similar shape as compared to the impact of increasing the destruction rate of eelgrass. Hence, we have fit the same model now having:

$$\bar{C}_{1,2}(\eta_{C_2}) = 0.1105 + \frac{1.2884}{1 + \exp(104.43\,(\eta_{C_2} - 0.084))}, \tag{3.2}$$

here with $R^2 = 0.986$. Parameter k in the logistic function is the steepness coefficient. That is, how pronounced are the changes in cod abundance around the threshold to the lowest values. Note that this sharpness coefficient is about 9-fold larger than the steepness coefficient due to the increase in eelgrass destruction. Hence, while the decrease in cod abundance is abrupt, increasing the destruction of eelgrass, the impact of fishing is even more dramatic.

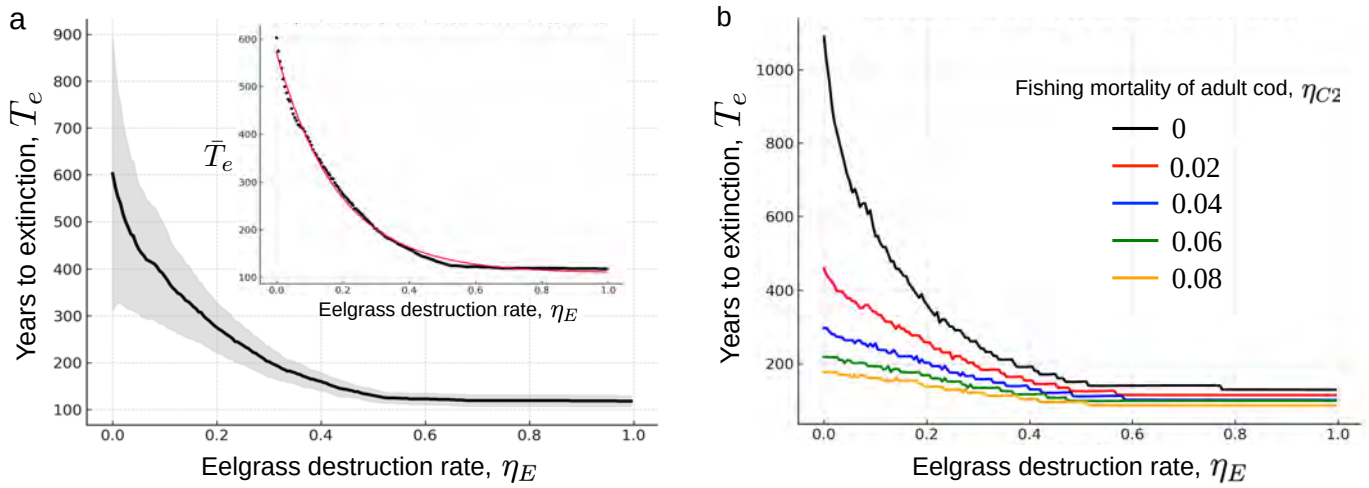

Figure S16: **Cod extinction times at varying levels of eelgrass destruction rate and fishing mortality of cod**. (a) Mean extinction times (black line) computed from 20 simulations using random cod natural mortality drawn from uniform distributions, with $\nu_{C1}, \nu_{C2} \in \text{rand}(0.25, 0.45)$ and $\omega_E = 1$. The grey area represents ± 1 SD. The inset shows the mean extinction times together with an exponential fit (red line). (b) Extinction times for the population of cod with cod natural mortality $\nu_{C1} = 0.3$ (juvenile) and $\nu_{C2} = 0.275$ (adult), at different levels of cod fishing mortality: $\eta_{C2} = 0$ (black); $\eta_{C2} = 0.02$ (red); $\eta_{C2} = 0.04$ (blue); $\eta_{C2} = 0.06$ (green); and $\eta_{C2} = 0.08$ (orange). The fishing mortality for juveniles has been set to $\eta_{C1} = \eta_{C2}/12.807$ [23]. The values of the other parameters are provided in Table S2.

Finally, we want to emphasise that the decrease of eelgrass abundance with increasing cod fishing mortality is also nonlinear: eelgrass area starts decreasing with an accelerated decrease towards a value close to the half of the carrying capacity for eelgrass.

We now evaluate how the destruction rate of eelgrass and the cod fishing mortality impact on the survival and persistence of the cod populations. To do so we have computed the times to extinction (or rather, collapse) of both juvenile and adult cod populations, according to the extinction thresholds defined in subection 1.3 above.

Figure 16(a) shows these times to extinction for cod populations, T_e, as a function of the eelgrass destruction rate, averaged over 20 simulations using random cod natural mortality drawn from uniform distributions. The extinction time is here considered the time at which both adults and juveniles have crossed the extinction threshold. The black line corresponds to the mean extinction time $\bar{T}_e$, while the shaded grey area represents the standard deviation (SD). This visualisation highlights both the central tendency and the variability of extinction times across replicates, providing a clear overview of the system's response. We did a fit of the mean extinction times using an exponential function. The inset in Figure 16(a) shows this fit. The mean values are shown as black points, and the fitted exponential curve is shown in red. This fitting was performed using non-linear least squares regression implemented in the `curve_fit` function from the `scipy.optimize` Python library. This method minimises the sum of squared residuals between the observed mean extinction times and the model prediction. The covariance matrix returned by the fit was used to estimate the standard errors of the parameters A, B, and C. The goodness-of-fit was quantified by the coefficient of determination (R^2), which measures the proportion of variance explained by the model. The fitting function was

$$\bar{T}_e(\eta_E) = A \exp(-B\,\eta_E) + C,$$

with best-fit parameters

$$A = 462.16 \pm 2.36, \quad B = 5.36 \pm 0.06, \quad C = 108.88 \pm 0.96.$$

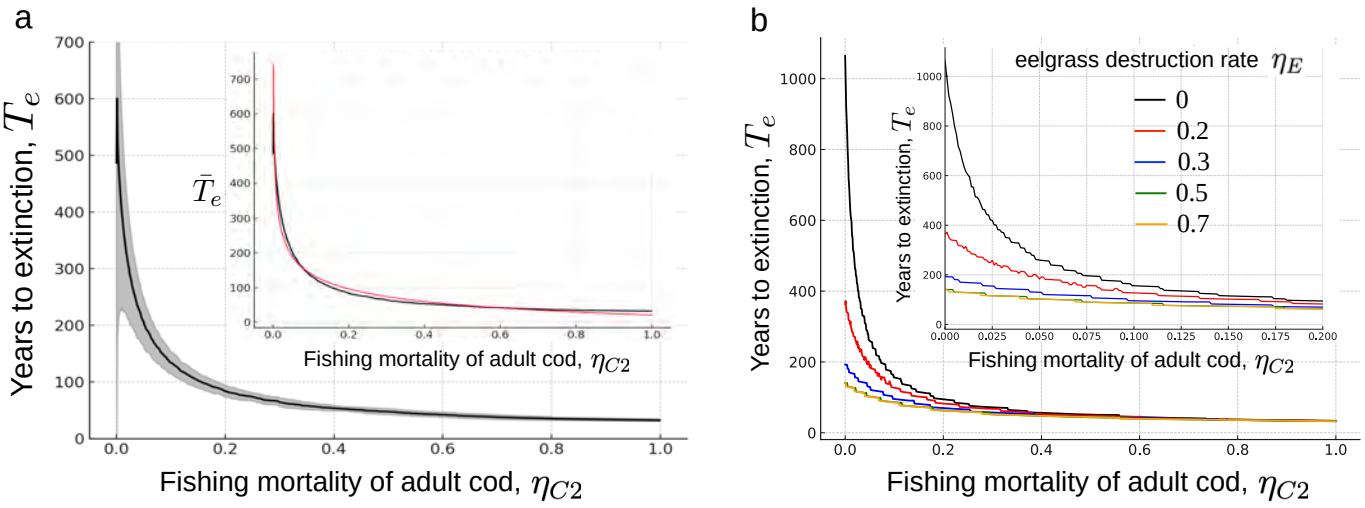

Figure S 17: **Cod extinction times at varying levels of cod fishing mortality**. (a) Mean extinction times (black line) for 20 simulations using random natural mortality with uniform distributions for cod populations, with $\nu_{C1}, \nu_{C2} \in \text{rand}\,(0.2, 0.4)$. The grey area shows $\pm$ 1 SD. The inset shows the mean time and a fit with a power-law model (red line). (b) Cod extinction times at varying levels of adult cod fishing mortality for different eelgrass destruction rates with $\nu_{C1} = 0.32$, $\nu_{C2} = 0.25$, and considering that the fishing mortality of juvenile cod is $\eta_{C1} = \eta_{C2}/12.807$ [23]. In all the simulations we have used $\omega_E = 1$. The values of the other parameters are provided in Table S2.

Here, A is the amplitude of the exponential decay, B is the decay rate, and C is the asymptotic extinction time at large parameter values. The fit achieved an R^2 of 0.996, indicating excellent agreement with the data.

Figure 16(b) shows the extinction times of cod populations for different levels of fishing mortality. Each curve corresponds to a different imposed fishing mortality, with extinction times plotted against the parameter values. The results demonstrate that extinction times decrease as fishing mortality increases. The curves exhibit a clear exponential-like decay, consistent across fishing intensities, although no explicit fitting functions are provided here.

Next, we investigate further how the extinction times change when increasing the fishing mortality of cod. Figure 17(a) shows the mean time to extinction $\bar{T}_e$ averaged over 20 simulations using random cod natural mortality drawn from uniform distributions as a black curve together with a grey band representing the SD.

To capture the systematic decay of the mean curve, we fitted exponential and power-law with an offset models. The power-law model fitted the data better, obtaining

$$\bar{T}_e(\eta_{C2}) \;=\; a\,\eta_{C2}^{-b} + c, \tag{3.3}$$

The fit was performed using non-linear least squares on the mean values (as explained above) for $\eta_{C2} > 0$ (the $\eta_{C2} = 0$ point was excluded to avoid the singularity of η_{C2}^{-b}). The inset in Figure 17(a) overlays the fitted curve (thin red line) on the empirical mean (black line). The power law provided an excellent description of the mean data with coefficient of determination $R^2 = 0.973$.

The estimated parameters (mean $\pm$ standard error from the covariance matrix of the fit) are:

$$\begin{aligned} a &= 147.52 \;\pm\; 4.54, \\ b &= 0.2566 \;\pm\; 0.0046, \\ c &= -126.61 \;\pm\; 4.93. \end{aligned}$$

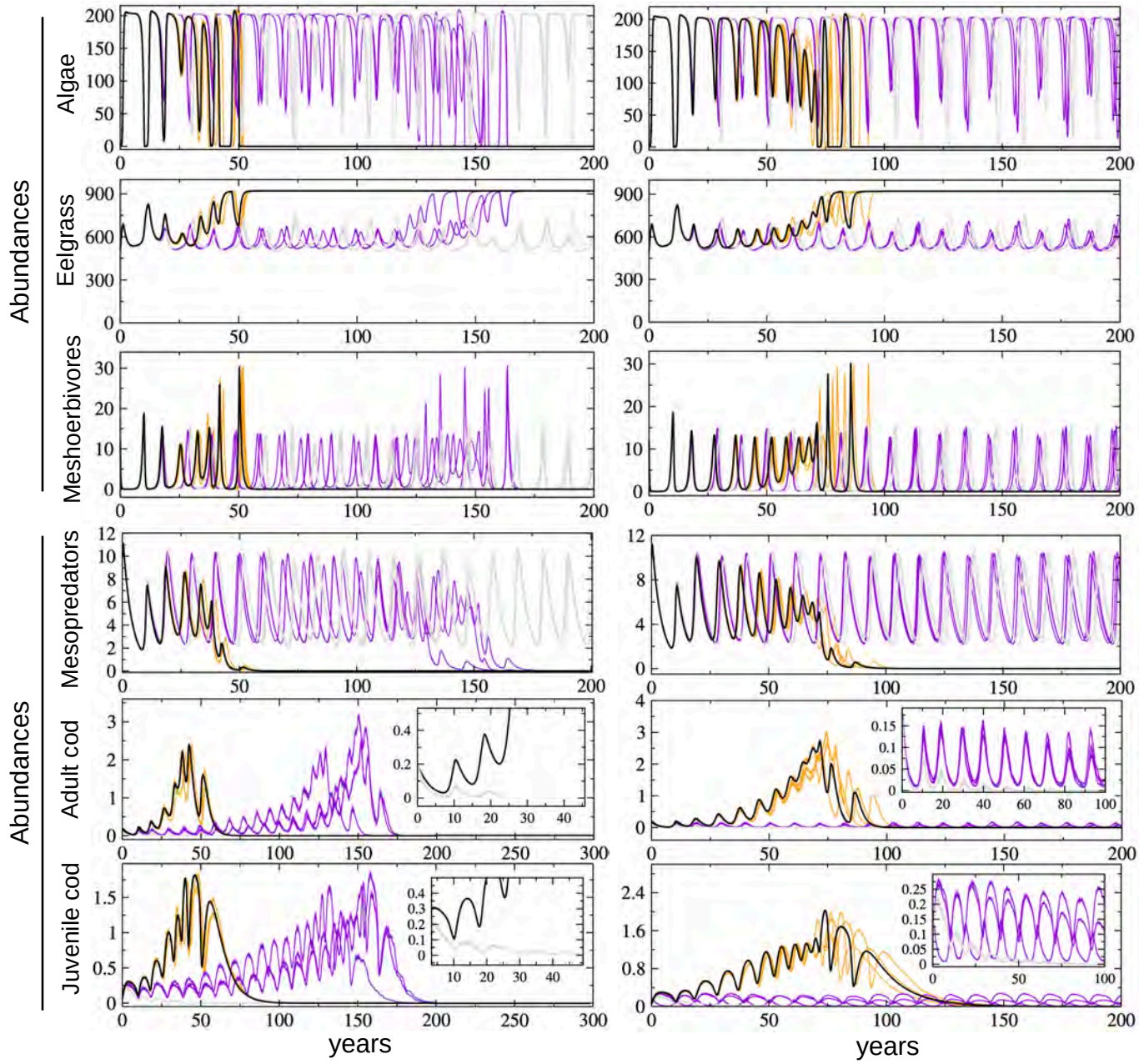

Figure S18: **Impact of environmental stochasticity on cod natural mortality rates on the entire trophic system**. The population dynamics for each trophic level is shown for the same cod natural mortality rates of Fig. S9(d-e), here with $\bar{\nu}_{C2} = 0.3$ and $\bar{\nu}_{C1} = 0.14$ (left panels); and $\bar{\nu}_{C2} = 0.42$ and $\bar{\nu}_{C1} = 0.08$ (right panels). Here we consider no eelgrass destruction ($\eta_E = 0$) and no fishing ($\eta_{C_2} = 0$). In all panels, the deterministic dynamics ($\sigma = 0$) is displayed with a thick black line. Overlapped to the deterministic case we display three stochastic realisations with $\sigma = 0.5$ (orange), and $\sigma = 1.5$ (violet); and $\sigma = 2.5$ (gray).

3.2.5 Stochastic dynamics: simulating the impact of environmental noise in cod natural death rates

Environmental stochasticity was incorporated by allowing the natural mortality rates of juvenile and adult cod, ν_{C1} and ν_{C2}, to fluctuate around their baseline values. The parameter σ controls the magnitude of these fluctuations, with larger values representing stronger environmental variability (see Section 2.5).

We focused stochasticity on cod mortality because it integrates multiple ecological processes not explicitly resolved in the model. In natural systems, survival of juvenile and adult cod varies due to temperature, oxygen availability, prey availability, disease, habitat conditions, and other stressors. These factors generate temporal deviations from mean mortality rates even when the trophic structure remains unchanged. Introducing stochasticity separately in ν_{C1} and ν_{C2} also reflects stage-specific responses: juveniles are typically more sensitive to recruitment conditions, habitat, and predation, whereas adult mortality is more influenced by physiological stress and disease. Stochastic mortality thus provides a simple and ecologically interpretable representation of environmental variability affecting cod persistence, with consequences for the entire trophic system.

We first explored the impact of stochasticity using the deterministic parameter values for cod natural mortality rates from Fig. S9(d–e). The results (Fig. S18) show that variability at the apex predator level strongly affects the entire system. For $\bar{\nu}_{C2} = 0.3$ and $\bar{\nu}_{C1} = 0.14$ (left panels), three noise amplitudes were considered: $\sigma = 0.5$ (orange), $\sigma = 1.5$ (violet), and $\sigma = 2.5$ (gray). These values correspond to increasing levels of variability in the mortality rates, from relatively small fluctuations around the mean, i.e., deterministic value, (approximately 50% variation) to strong deviations exceeding 200%, thereby spanning a broad range of environmental variability.

For $\sigma = 0.5$, the dynamics remain close to the deterministic case (thick black line) across all trophic levels. Increasing σ generally leads to a stabilization of the dynamics and delays cod extinction. In the deterministic case, cod populations go extinct after approximately 100 years, whereas under moderate noise ($\sigma = 1.5$) extinction occurs later, around 175–200 years. In contrast, large noise amplitudes ($\sigma = 2.5$) lead to rapid cod extinction (see insets), although lower trophic levels remain persistent and more stable.

A similar pattern is observed for $\bar{\nu}_{C2} = 0.42$ and $\bar{\nu}_{C1} = 0.08$ (right panels in Fig. S18). For $\sigma = 0.5$, the dynamics closely follow the deterministic case. For intermediate noise ($\sigma = 1.5$), the system stabilizes and cod populations persist at low abundances for very long times (on the order of thousands of years). However, for higher noise levels ($\sigma = 2.5$), cod populations rapidly go extinct, while the remaining trophic levels continue to exhibit persistent fluctuations. For this latter case, the extinction times of both adult and juvenile cod are found after 100 years approximately, as a difference from the simulations carried out in Fig. S18, left panels. This difference could be given by the lowest mortality rate of juvenile cod ($\bar{\nu}_{C1} = 0.08$). Despite the mortality of adult cod is large, the lower mortality of juvenile cod could sustein the cod population for longer times.

Next, we examine the interplay between noise levels on cod natural mortality, cod fishing, and eelgrass destruction. To do so, we have simulated the dynamics of the system for the same three noise amplitudes previously used, together with increasing adult cod fishing rates. For each of these scenarios, we compare the dynamics considering no eelgrass destruction and eelgrass destruction (using $\eta_E = 0.9$). The results are displayed in Fig. S19 by means of cod time series. Here, we have set the baseline natural death rates of cod at low values, i.e., $\bar{\nu}_{C2} = 0.1$, $\bar{\nu}_{C1} = 0.15$, but considering higher mortality of juveniles, to promote cod persistence and evaluate the impact of fishing and eelgrass destruction.

When the fishing rate of adult cod is low ($\eta_{C_2} = 0.1$) and no eelgrass destruction is considered, cod populations initially increase with strong fluctuations, but both adult and juvenile cod collapse after approximately 50 years. A similar scenario is observed when eelgrass destruction is included. In this case, juvenile cod reach lower abundances, and their collapse occurs later, at around 100 years,

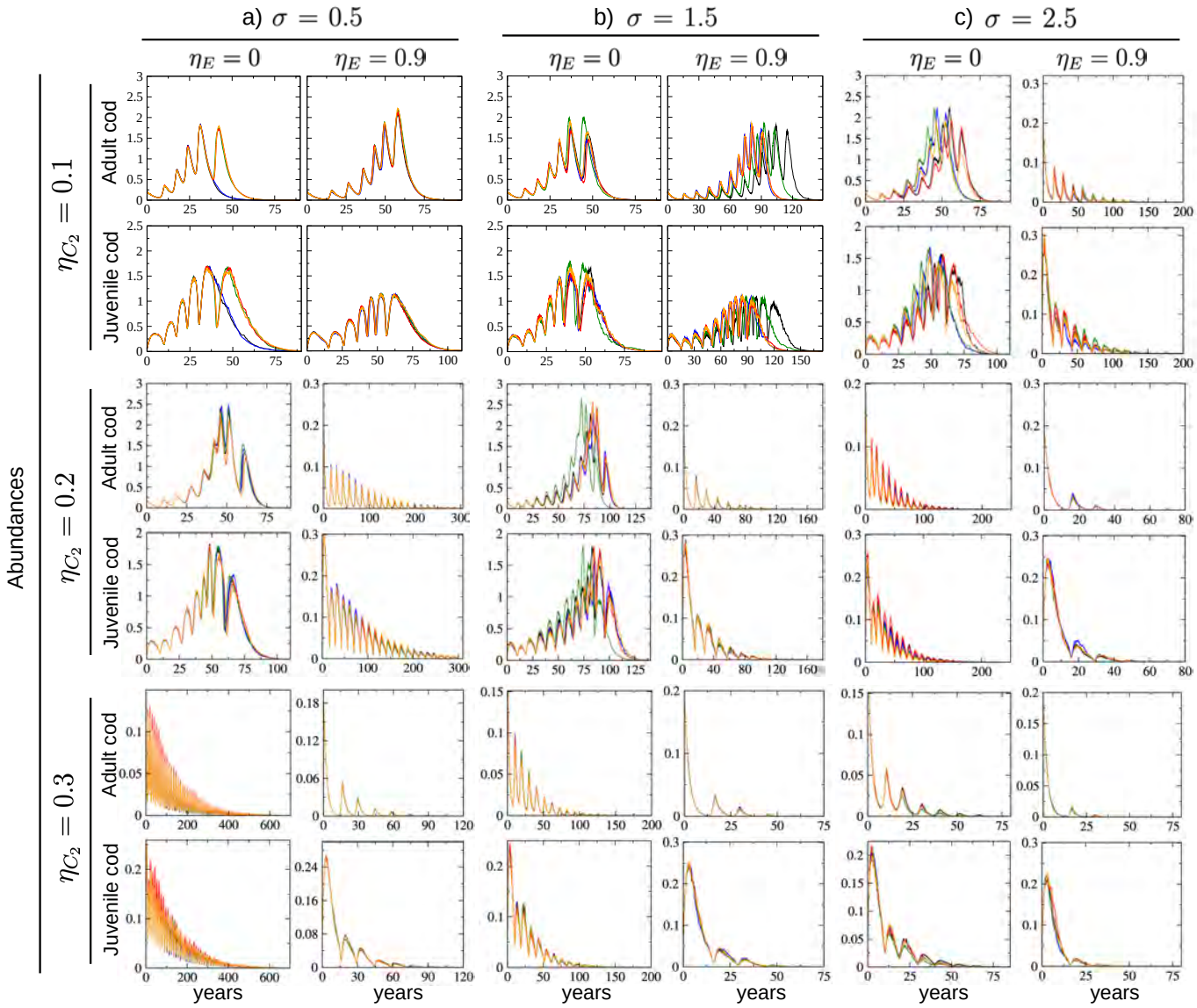

Figure S 19: **Impact of environmental stochasticity on cod natural death rates and its interaction with fishing and eelgrass destruction**. Dynamics of adult and juvenile cod at increasing the environmental noise on their natural death rates setting $\bar{\nu}_{C2} = 0.1$, $\bar{\nu}_{C1} = 0.15$. Three cases increasing the fishing rates of adult cod are shown: $\eta_{C_2} = 0.1$, $\eta_{C_2} = 0.2$, and $\eta_{C_2} = 0.3$. For each case, we have simulated different noise amplitudes with $\sigma = 0.5$ (a), $\sigma = 1.5$ (a), and $\sigma = 2.5$ (a). Each panel displays five stochastic simulations with no eelgrass degradation ($\eta_E = 0$) and with an eelgrass destruction rate of $\eta_E = 0.9$.

followed by the collapse of adult cod.

Increasing the noise amplitude to $\sigma = 1.5$ leads to qualitatively similar dynamics. As discussed previously, stochasticity tends to stabilize the system and delay extinction. In the absence of eelgrass destruction, cod populations collapse after approximately 80 years, whereas with eelgrass destruction, extinction is delayed to around 150 years. Although this might suggest that eelgrass destruction promotes longer persistence times for cod, this effect is likely driven by the reduction in juvenile cod abundance, which weakens trophic interactions and allows both juvenile and adult populations to persist longer at low densities.

For larger noise amplitudes ($\sigma = 2.5$), and in the absence of eelgrass destruction, adult cod exhibit dynamics similar to those observed at lower noise levels, while juvenile populations decline, with both stages collapsing after approximately 90 years. However, when eelgrass destruction is included, both adult and juvenile cod experience a substantial reduction in abundance (by factors of approximately 15 and 10, respectively), followed by a sustained decline until extinction occurs at around 160 years. In this case, the low cod densities likely also exert weaker top-down control on lower trophic levels, thereby reducing feedback pressures and allowing cod populations to persist longer before eventual collapse.

Increasing the fishing mortality of adult cod further amplifies the interaction with eelgrass dynamics. Simulations with $\eta_{C_2} = 0.2$, $\sigma = 0.5$ (Fig. S19), and no eelgrass destruction show patterns similar to those observed at lower fishing rates. However, when eelgrass destruction is included, the dynamics change markedly. Both adult and juvenile cod populations decline substantially and approach extinction through oscillatory dynamics. Due to the low abundances, collapse occurs only after approximately 350 years.

When the noise amplitude is increased to $\sigma = 1.5$, cod populations initially recover but eventually collapse after approximately 125 years. In the presence of eelgrass destruction, both populations again fluctuate at very low abundances before going extinct. Further increases in noise amplitude drive cod populations to extinction both with and without eelgrass destruction. However, the time to collapse is reduced by more than half when eelgrass is destroyed.

Finally, for higher fishing mortality ($\eta_{C_2} = 0.3$), cod populations fluctuate at very low abundances and move toward extinction under all scenarios considered (Fig. S19). As noted above, cases with eelgrass destruction substantially accelerate the timing of cod collapse.

Overall, the transient cod persistence is affected by the interaction between environmental variability, fishing pressure, and eelgrass condition. Moderate noise and eelgrass destruction can delay collapse because cod abundances remain at very low values. Increased fishing pressure also reduces cod populations substantially, causing a sustained decline towards collapse, which is further accelerated if eelgrass is destroyed.

3.2.6 Sensitivity analysis using Monte Carlo

Figures S20–S24 present the results of randomized simulations, in which parameter values were sampled within a prescribed interval corresponding to a 30% uncertainty range. This approach was used to assess the robustness of the model's predictions.

We emphasize that these simulations do not represent stochastic dynamics as considered in the previous section. Instead, they correspond to a sensitivity analysis based on a Monte Carlo sampling of the parameter space. In this framework, parameters are randomly drawn but remain fixed throughout each simulation; that is, they do not vary in time. This allows us to explore a broader region of parameter space and evaluate the consistency of our results and conclusions under parametric uncertainty.

Despite the added uncertainties, the overall qualitative patterns remain largely consistent with those described above for the deterministic baseline. In all cases, the main trophic structure and the relative dominance of the different functional groups are preserved. This indicates that the emergent

dynamics are not artifacts of specific parameter combinations but rather intrinsic to the model's formulation and interactions among trophic levels.

Figures S20 shows that the abundance diagrams computed in Figure 5 in the main manuscript remain under the randomised parameters. That is, the populations of cod substantially decrease with increasing cod mortality. Those regions with the largest cod abundances also coincide with the most extensive eelgrass areas and lower mesopredator and algae abundances. These results remain when increasing the destruction rate of eelgrass (see panels for $\eta_E = 0.85$ in Figure S20), with lower mean abundances of both adult and juvenile cod. Moreover, all the other trophic levels show lower abundances, except the filamentous algae.

Figure S21 shows the sensitivity analysis performed on the same parameter space as in Figure S8. The randomised diagrams indeed show that cod is fragile to increased mortality, with the mortality of adult cod being more critical to cod persistence. In agreement with the previous results, the cod mortality supporting larger cod populations involves wider eelgrass areas and lower algae abundances. The top-down control of cod populations on mesopredators is clearly visible in the abundance of mesopredators. However, the mean populations for the randomised ensembles are generally lower than those obtained with the fixed parameters. Similar results are obtained for the other randomised phase diagrams (see Figs. S22-S24).

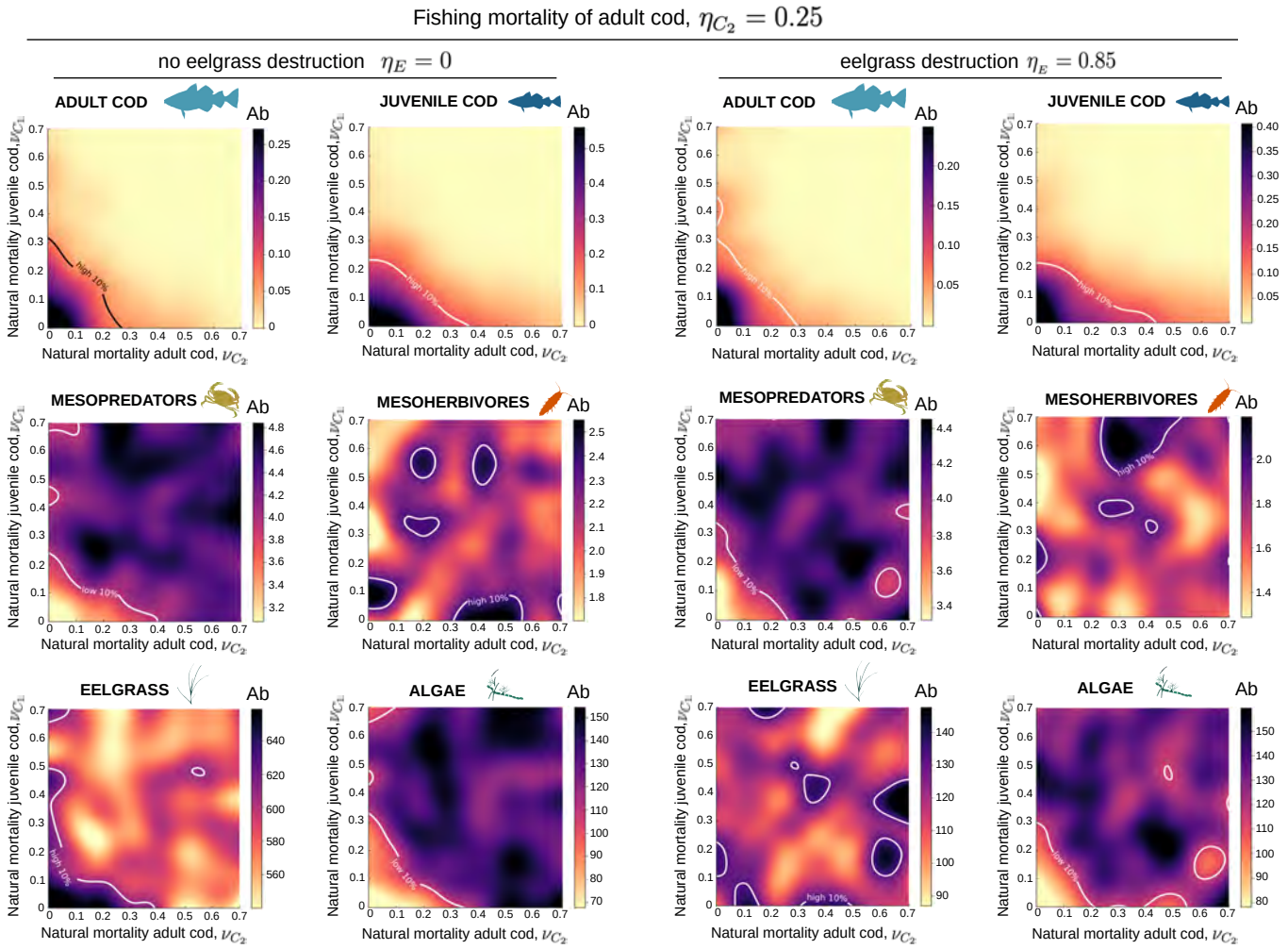

Figure S20: **Sensitivity analysis of the abundance diagrams tuning cod natural mortality**. Here we explore the same parameter space shown in Figure 5 in the main manuscript with $\omega_E = 1$, setting all the other parameters at random within the ranges given in Table S2. Adult fishing mortality η_{C2} is set to 0.25, and eelgrass destruction rate η_E is set to 0 in the left set of plots, and 0.85 in the right set of plots. Note that the explored ranges for ν_{C_1} and ν_{C_2} are wider than in Figure 5 in the main manuscript. The contour lines indicate regions corresponding to extreme abundance values: the highest 10% for cod, mesoherbivores, and eelgrass; and the lowest 10% for mesopredators and filamentous algae.

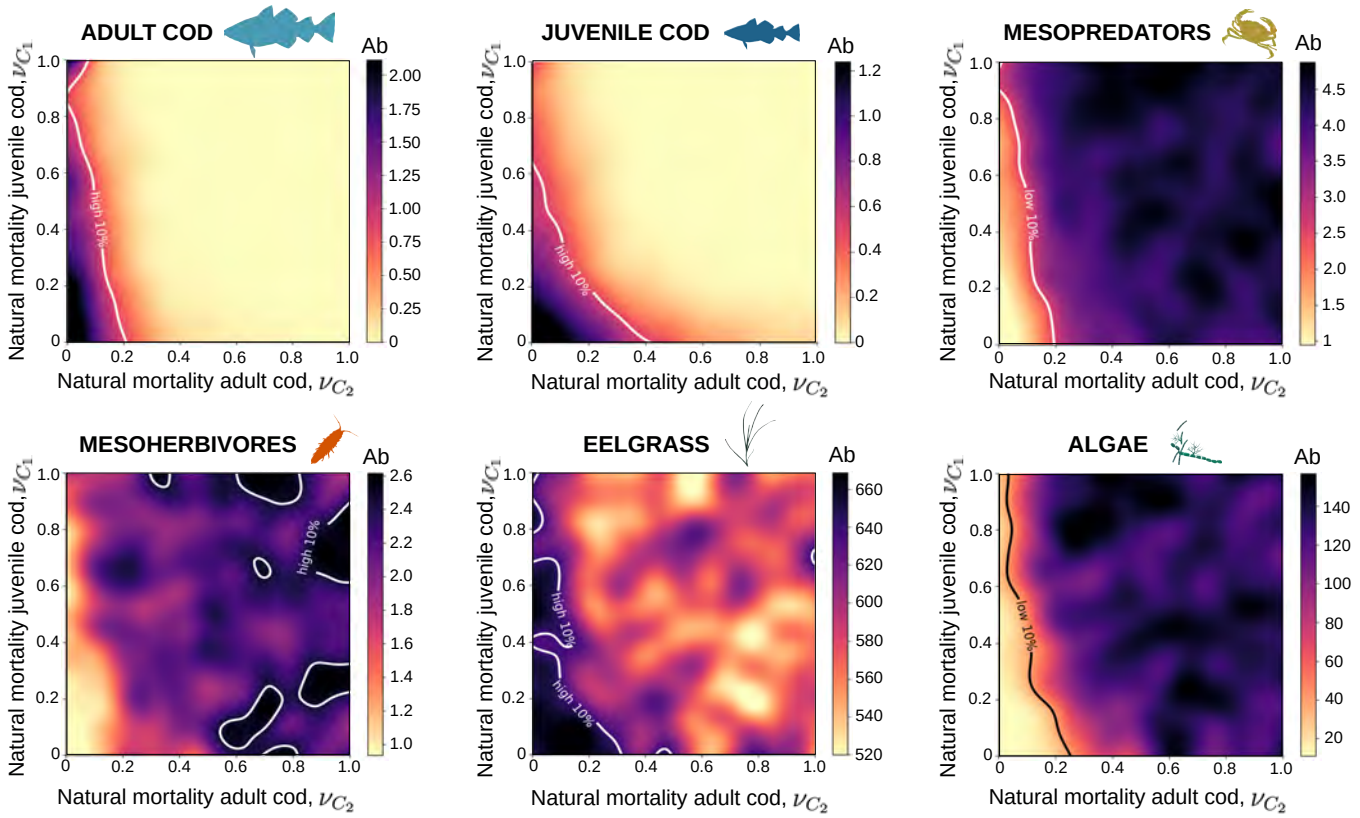

Figure S 21: **Sensitivity analysis of the abundance diagrams tuning cod natural mortality with no cod fishing**. Here we explore the same parameter space shown in Figure S8 using the randomised parameter ensembles. The contour lines indicate regions corresponding to extreme abundance values: the highest 10% for cod, mesoherbivores, and eelgrass; and the lowest 10% for mesopredators and filamentous algae.

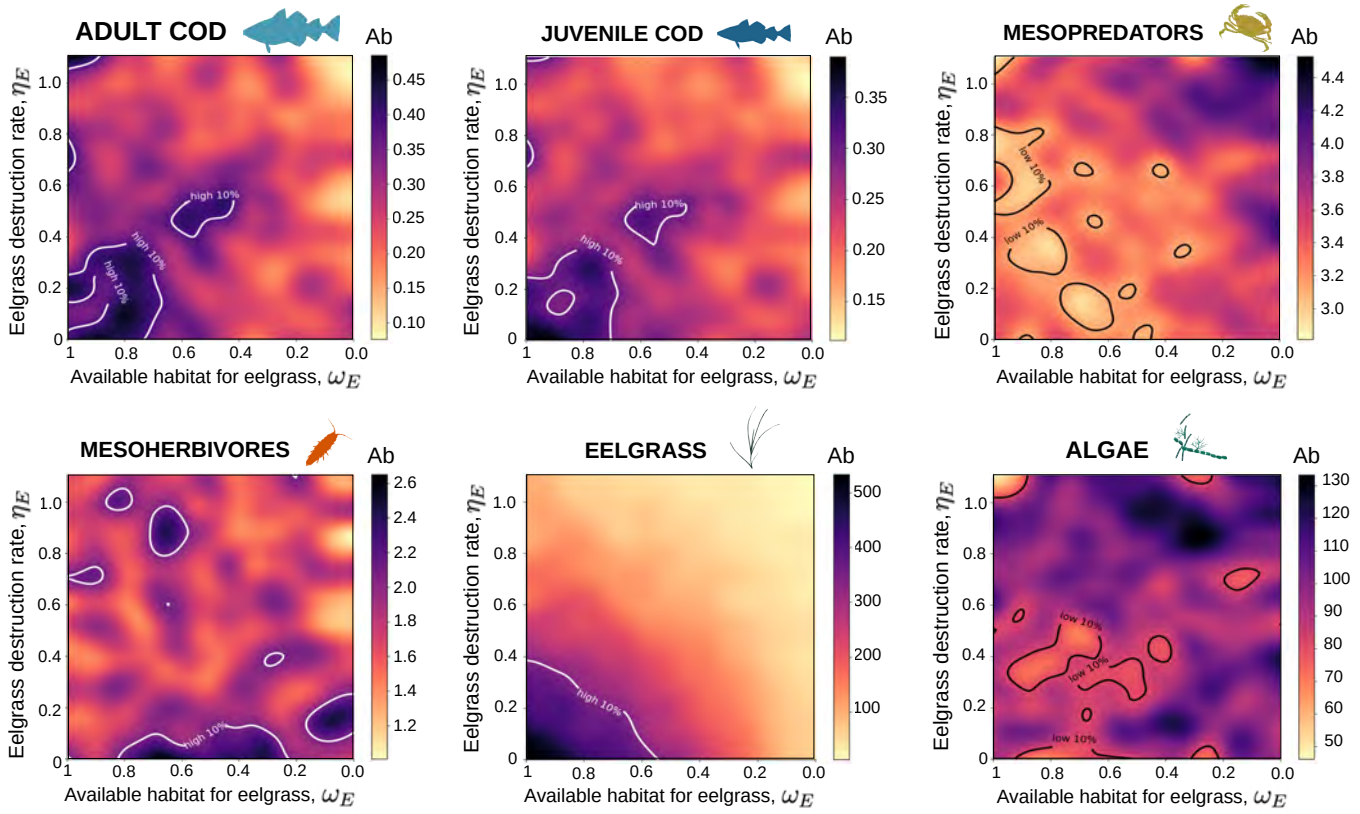

Figure S 22: **Sensitivity analysis of the abundance diagrams tuning eelgrass destruction rate and the amount of available habitat**. Here we explore the same parameter space shown in Figure S11 using the randomised parameter ensembles. The contour lines indicate regions corresponding to extreme abundance values: the highest 10% for cod, mesoherbivores, and eelgrass; and the lowest 10% for mesopredators and filamentous algae.

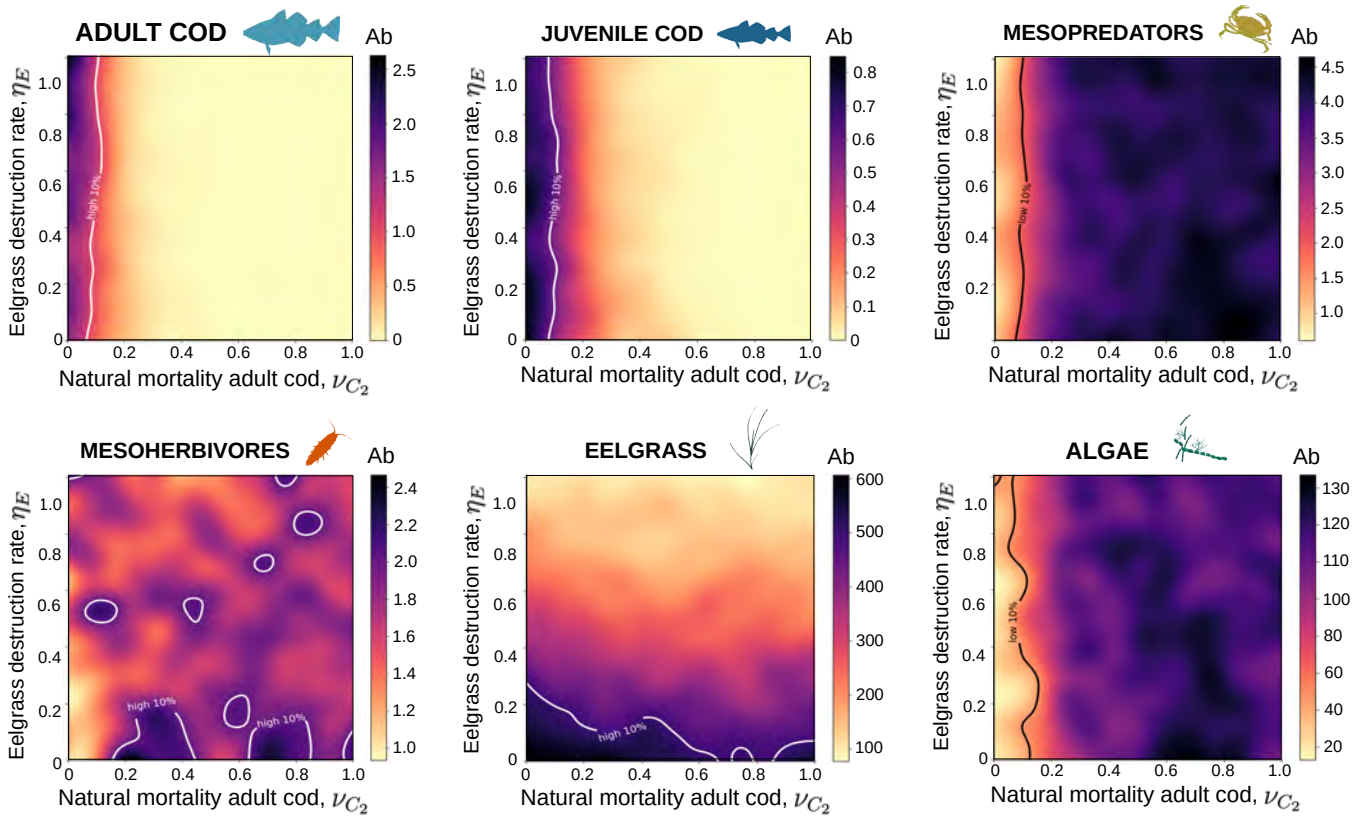

Figure S 23: **Sensitivity analysis of the abundance diagrams tuning eelgrass destruction rate and the natural mortality of adult cod**. Here we explore the same parameter space shown in Figure S12 using the randomised parameter ensembles. The contour lines indicate regions corresponding to extreme abundance values: the highest 10% for cod, mesoherbivores, and eelgrass; and the lowest 10% for mesopredators and filamentous algae.

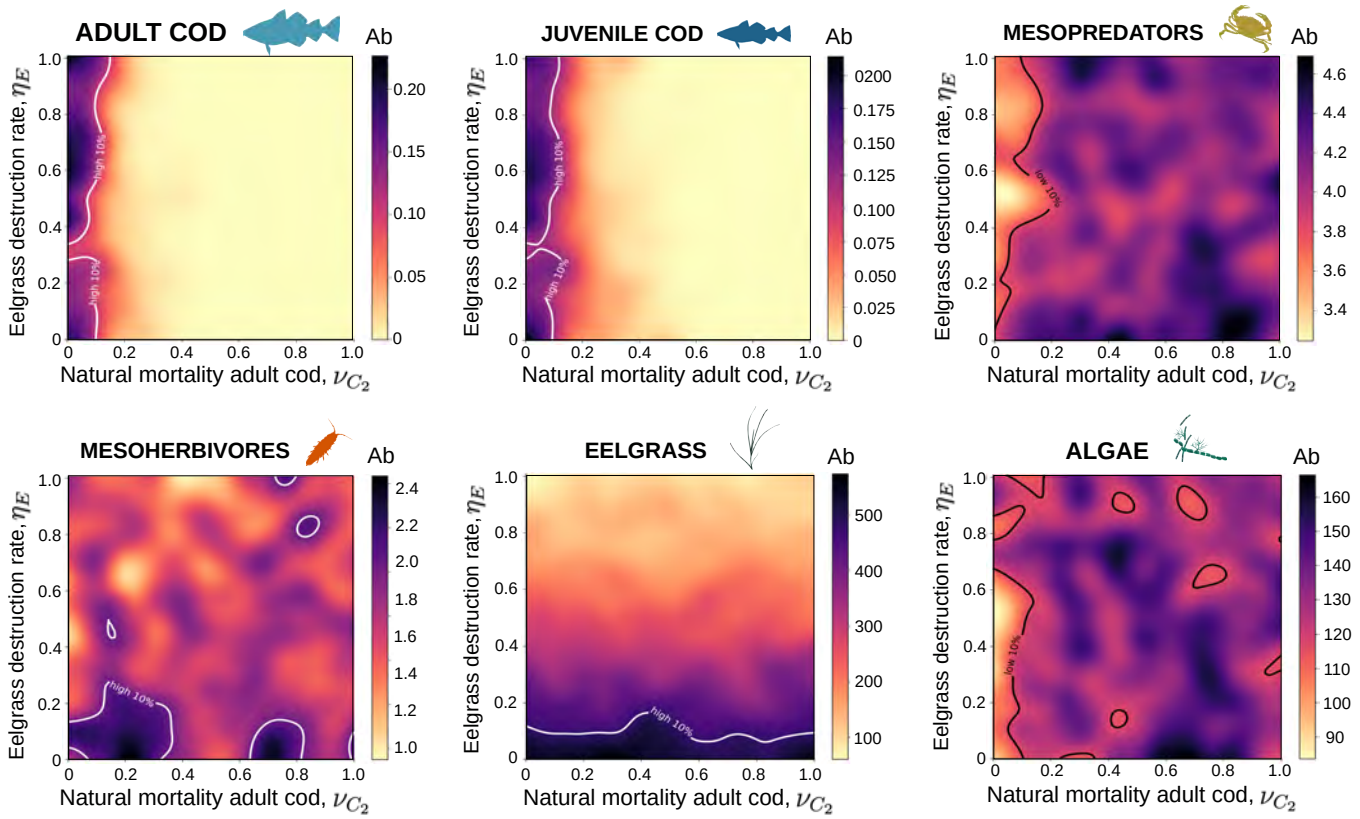

Figure S 24: **Sensitivity analysis of the abundance diagrams tuning eelgrass destruction rate and the natural mortality of adult cod**. Here we explore the same parameter space shown in Figure S13, but setting $\omega_E = 1$ and using the randomised parameter ensembles. The contour lines indicate regions corresponding to extreme abundance values: the highest 10% for cod, mesoherbivores, and eelgrass; and the lowest 10% for mesopredators and filamentous algae.

References

[1] Baden, S., Boström, C., Tobiasson, S., Arponen, H., Moksnes, P.O.: Relative importance of trophic interactions and nutrient enrichment in seagrass ecosystems: A broad-scale field experiment in the Baltic–Skagerrak area. Limnology and oceanography **55**, 1435–1448 (2010). DOI 10.4319/lo.2010.55.3.1435

[2] Baden, S., Emanuelsson, A., Pihl, L., Svensson, C., Aberg, P.: Shift in seagrass food web structure over decades is linked to overfishing. Marine Ecology Progress Series **451**, 61–73 (2012). DOI 10.3354/meps09585

[3] Barr, N., Rees, T.: Nitrogen status and metabolism in the green seaweed Enteromorpha intestinalis: an examination of three natural populations. Marine Ecology Progress Series **249**, 133–144 (2003). DOI 10.3354/meps249133

[4] Barr, N., Rees, T.: Nitrogen status and metabolism in the green seaweed Enteromorpha intestinalis: An examination of three natural populations. Marine Ecology Progress Series **249**, 133–144 (2003). DOI 10.3354/meps249133

[5] Berglund, J., Thomasdotter, A., Paz von Friesen, C., Åkerholm, M., Saarinen, A., Nordling, P., Kraft, E., Danbolt, M., Wall, A., Infantes, E., Envall, M., Möller, H., Rasmussen, M., Moksnes, P.O.: Marin Fjärranalys – Övervakning av vegetationsutbredning med satelliter och drönare. Tech. rep., Länsstyrelsen Västerbotten (2023)

[6] Bergström, L., Jansson, M., Sundqvist, F., Andersson, J.: Biologiska undersökningar vid Ringhals kärnkraftverk 1979–2007. Fiskeriverket Informerar **2**, 1–37 (2009)

[7] Borum, J., Duarte, C., Krause-Jensen, D., Greve, T.: European Seagrasses: An Introduction to Monitoring and Management. The M& MS project (2004)

[8] Charrieau, L., Ljung, K., Schenk, F., Daewel, U., Kritzberg, E., Filipsson, H.: Rapid environmental responses to climate-induced hydrographic changes in the Baltic Sea entrance. Biogeosciences Discussions pp. 1–45 (2019). DOI 10.5194/bg-2019-199

[9] Costa, F.O., Costa, M.H.: Life history of the amphipod Gammarus locusta in the Sado estuary (Portugal). Acta Oecologica **20**(4), 305–314 (1999). DOI 10.1016/S1146-609X(99)00136-8

[10] Defaveri, J., Merilä, J.: Variation in Age and Size in Fennoscandian Three-Spined Sticklebacks (Gasterosteus aculeatus). PloS one **8**, e80866 (2013). DOI 10.1371/journal.pone.0080866

[11] van Deurs, M., Persson, A., Nilsson, P.A., Jørgensen, C.: Fish resist temptation from junk food: state-dependent diet choice in reproductive Atlantic cod Gadus morhua facing seasonal fluxes of lipid-rich prey. Oikos **2022**(7) (2022). DOI 10.1111/oik.08739

[12] Eilola, K., Stigebrandt, A.: Modelling filamentous algae mats in shallow bays. Tech. rep., Göteborg University (2014)

[13] Froese, R.: Search FishBase (2024). URL `https://fishbase.mnhn.fr/search.php`

[14] Funk, S., Frelat, R., Möllmann, C., Temming, A., Krumme, U.: The forgotten feeding ground: patterns in seasonal and depth-specific food intake of adult cod Gadus morhua in the western Baltic Sea. Journal of Fish Biology **98**(3), 707–722 (2021). DOI 10.1111/jfb.14615

[15] Funk, S., Funk, N., Herrmann, J.P., Hinrichsen, H.H., Krumme, U., Möllmann, C., Temming, A.: Tracing growth patterns in cod (Gadus morhua L.) using bioenergetic modelling. Ecology and Evolution **13**(11), e10751 (2023). DOI https://doi.org/10.1002/ece3.10751

[16] Gagnon, K., Gräfnings, M., Boström, C.: Trophic role of the mesopredatory three-spined stickleback in habitats of varying complexity. Journal of Experimental Marine Biology and Ecology **510**, 46–53 (2019). DOI 10.1016/j.jembe.2018.10.003

[17] Garbary, D.J., Miller, A.G., Williams, J., Seymour, N.R.: Drastic decline of an extensive eelgrass bed in Nova Scotia due to the activity of the invasive green crab (Carcinus maenas). Marine Biology **161**(1), 3–15 (2014). DOI 10.1007/s00227-013-2323-4

[18] Gogina, M., Zettler, A., Zettler, M.L.: Weight-to-weight conversion factors for benthic macrofauna: recent measurements from the Baltic and the North seas. Earth System Science Data **14**(1), 1–4 (2022). DOI 10.5194/essd-14-1-2022

[19] Gras, A., Koch, M.: Phosphorus uptake kinetics of a dominant tropical seagrass. Aquatic Botany **76**, 299–315 (2003)

[20] Grønkjær, P., Clemmesen, C., John, M.: Nutritional condition and vertical distribution of Baltic cod larvae. Journal of Fish Biology **51**, 352–369 (2006). DOI 10.1111/j.1095-8649.1997.tb06108.x

[21] Hinrichsen, H.H., Böttcher, U., Köster, F.W., Lehmann, A., St.John, M.A.: Modelling the influences of atmospheric forcing conditions on Baltic cod early life stages: distribution and drift. Journal of Sea Research **49**(3), 187–201 (2003). DOI 10.1016/S1385-1101(03)00006-6

[22] Huber, S., Hansen, L.B., Nielsen, L.T., Rasmussen, M.L., Sølvsteen, J., Berglund, J., Paz von Friesen, C., Danbolt, M., Envall, M., Infantes, E., Moksnes, P.: Novel approach to large-scale monitoring of submerged aquatic vegetation: A nationwide example from Sweden. Integrated Environmental Assessment and Management **18**(4), 909–920 (2022). DOI 10.1002/ieam.4493

[23] ICES: Baltic Fisheries Assessment Working Group (WGBFAS). report, ICES Scientific Reports (2023). DOI 10.17895/ices.pub.23123768.v1. URL `https://ices-library.figshare.com/articles/report/Baltic_Fisheries_Assessment_Working_Group_WGBFAS_/23123768/1?file=43164541`. Visited on 2024-07-18

[24] ICES: Cod (Gadus morhua) in Subdivision 21 (Kattegat). Tech. rep., ICES Advice: Recurrent Advice (2024). DOI doi:10.17895/ices.advice.25019213.v2

[25] ICES: Cod (Gadus morhua) in subdivisions 22-24, western Baltic stock (western Baltic Sea). ICES Advice 2023 (2025)

[26] ICES: Cod (Gadus morhua) in subdivisions 22-24, western Baltic stock (western Baltic sea). Tech. rep., ICES Advice: Recurrent Advice (2025). DOI doi:10.17895/ices.advice.27202560.v1

[27] Infantes, E., Crouzy, C., Moksnes, P.O.: Seed Predation by the Shore Crab Carcinus maenas: A Positive Feedback Preventing Eelgrass Recovery? PLOS ONE **11**(12), e0168128 (2016). DOI 10.1371/journal.pone.0168128

[28] Unit conversions (2024). URL `https://www.ices.dk/data/tools/Pages/Unit-conversions.aspx`. Visited on 2024-05-24

[29] Jephson, T., Nyström, P., Moksnes, P., Baden, S.: Trophic interactions in Zostera marina beds along the Swedish coast. Marine Ecology Progress Series **369**, 63–76 (2008). DOI 10.3354/meps07646

[30] Jobling, M.: A review of the physiological and nutritional energetics of cod, Gadus morhua L., with particular reference to growth under farmed conditions. Aquaculture **70**(1), 1–19 (1988). DOI 10.1016/0044-8486(88)90002-6

[31] Koehler, B., Erlandsson, M., Karlsson, M., Bergström, L.: Species richness and functional attributes of fish assemblages across a large-scale salinity gradient in shallow coastal areas. Biogeosciences **19**(8), 2295–2312 (2022). DOI 10.5194/bg-19-2295-2022. Publisher: Copernicus GmbH

[32] Lapointe, B.E., Tenore, K.R.: Experimental outdoor studies with Ulva fasciata Delile. I. Interaction of light and nitrogen on nutrient uptake, growth, and biochemical composition. Journal of Experimental Marine Biology and Ecology **53**(2), 135–152 (1981). DOI 10.1016/0022-0981(81)90015-0

[33] Laurence, G.C., Rogers, C.A.: Effects of temperature and salinity on comparative embryo development and mortality of Atlantic cod (Gadus morhua L.) and haddock (Melanogrammus aeglefinus (L.)). ICES Journal of Marine Science **36**(3), 220–228 (1976). DOI 10.1093/icesjms/36.3.220

[34] Lawton, R., de Nys, R., Paul, N.: Selecting Reliable and Robust Freshwater Macroalgae for Biomass Applications. PloS one **8**, e64168 (2013). DOI 10.1371/journal.pone.0064168

[35] Lawton, R.J., De Nys, R., Paul, N.A.: Selecting Reliable and Robust Freshwater Macroalgae for Biomass Applications. PLoS ONE **8**(5), e64168 (2013). DOI 10.1371/journal.pone.0064168

[36] Lepoint, G., O., D., Gobert, S., Dauby, P., Bouquegneau, J.M.: Experimental evidence for n recycling in the leaves of the seagrass . J. Sea Research **48**, 173–179 (2006)

[37] Lilley, R., Unsworth, R.: Atlantic cod (Gadus morhua) benefits from the availability of seagrass (Zostera marina) nursery habitat. Global Ecology and Conservation **2**, 367–377 (2014). DOI 10.1016/j.gecco.2014.10.002

[38] Linehan, J., Gregory, R., Schneider, D.: Predation risk of age-0 cod (Gadus) relative to depth and substrate in coastal waters. Journal of Experimental Marine Biology and Ecology **263**, 25–44 (2001). DOI 10.1016/S0022-0981(01)00287-8

[39] Ljungberg, P., Nilsson, A., Persson, A.: Prey selectivity by juvenile Atlantic cod (Gadus morhua) in three coastal habitat types. Marine Ecology Progress Series **466**, 215–223 (2012). DOI 10.3354/meps09932

[40] Mateo, I.: A Bioenergetics Based Comparison of Growth Conversion Efficiency of Atlantic Cod on Georges Bank and in the Gulf of Maine. Journal of Northwest Atlantic Fishery Science **38** (2007). DOI 10.2960/J.v38.m590

[41] Moksnes, P.O., Gullström, M., Tryman, K., Baden, S.: Trophic cascades in a temperate seagrass community. Oikos **117**(5), 763–777 (2008). DOI 10.1111/j.0030-1299.2008.16521.x

[42] Monteiro, J.N., Ovelheiro, A., Ventaneira, A.M., Vieira, V., Teodósio, M.A., Leitão, F.: Variability in Carcinus maenas Fecundity Along Lagoons and Estuaries of the Portuguese Coast. Estuaries and Coasts **45**(6), 1716–1727 (2022). DOI 10.1007/s12237-021-01035-9

[43] Nadaraya, E.A.: On estimating regression. Theory of Probability and its Applications **9**(1), 141–142 (1964). DOI 10.1137/1109020

[44] Neal, K., Pizzola, P.: Common shore crab (Carcinus maenas): Marine Evidence–based Sensitivity Assessment (MarESA) Review (2024). DOI 10.17031/MARLINSP.1497.2. URL `{http://www.marlin.ac.uk/assets/pdf/species/marlin\_species\_1497\_2019\-03\-21.pdf}`. Visited on 2024-08-24

[45] Neuenfeldt, S., Bartolino, V., Orio, A., Andersen, K., Andersen, N., Niiranen, S., Bergström, U., Ustups, D., Kulatska, N., Casini, M.: Feeding and growth of Atlantic cod (Gadus morhua L.) in the eastern Baltic Sea under environmental change. ICES Journal of Marine Science **77**, 624–632 (2020). DOI 10.1093/icesjms/fsz248

[46] Neuenfeldt, S., Bartolino, V., Orio, A., Andersen, K., Andersen, N., Niiranen, S., Bergström, U., Ustups, D., Kulatska, N., Casini, M.: Feeding and growth of Atlantic cod (Gadus morhua L.) in the eastern Baltic Sea under environmental change. ICES Journal of Marine Science **77**, 624–632 (2020). DOI 10.1093/icesjms/fsz248

[47] Nielsen, J.R., Lundgren, B., Jensen, T., Stæhr, K.J.: Distribution, density and abundance of the western Baltic herring (Clupea harengus) in the Sound (ICES Subdivision 23) in relation to hydrographical features. Fisheries Research **50**, 235–258 (2001). DOI 10.1016/S0165-7836(00)00220-4

[48] Nielsen, O., Koch, M., Jensen, H., Madden, C.: Thalassia testudinum phosphate uptake kinetics at low in situ concentrations using a 33P radioisotope technique. Limnology and Oceanography - LIMNOL OCEANOGR **51**, 208–217 (2006). DOI 10.4319/lo.2006.51.1.0208

[49] Pedersen, M., Borum, J.: Nitrogen dynamics of eelgrass Zostera marina during late summer period of high growth and low nutrient availability. Marine Ecology Progress Series **80**, 65–73 (1992). DOI 10.3354/meps080065

[50] Pihl, L., Baden, S., Kautsky, N., Rönnbäck, P., Svedäng, H., Troell, M., Wennhage, H.: Shift in fish assemblage structure due to loss of seagrass Zostera marina habitats in Sweden. Estuarine, Coastal and Shelf Science **67**(1-2), 123–132 (2006)

[51] Pihl, L., Isaksson, I., Wennhage, H., Moksnes, P.O.: Recent increase of filamentous algae in shallow Swedish bays: Effects on the community structure of epibenthic fauna and fish. Netherland Journal of Aquatic Ecology **29**(3), 349–358 (1995). DOI 10.1007/BF02084234

[52] Pihl, L., Rosenberg, R.: Production, abundance, and biomass of mobile epibenthic marine fauna in shallow waters, Western Sweden. Journal of Experimental Marine Biology and Ecology **57**(2), 273–301 (1982). DOI 10.1016/0022-0981(82)90197-6

[53] Rasmussen, J., Olesen, B., Krause-Jensen, D.: Effects of filamentous macroalgae mats on growth and survival of eelgrass, Zostera marina, seedlings. Aquatic Botany **99**, 41–48 (2012). DOI 10.1016/j.aquabot.2012.01.005

[54] Rasmussen, J., Pedersen, M., Olesen, B., Nielsen, S., Pedersen, T.: Temporal and spatial dynamics of ephemeral drift-algae in eelgrass, Zostera marina, beds. Estuarine, Coastal and Shelf Science **119**, 167–175 (2013). DOI 10.1016/j.ecss.2013.01.006

[55] Strong, K.W., Daborn, G.R.: Growth and energy utilisation of the intertidal isopod Idotea baltica (Pallas) (Crustacea: Isopoda). Journal of Experimental Marine Biology and Ecology **41**(2), 101–123 (1979). DOI 10.1016/0022-0981(79)90046-7

[56] Sutcliffe, D.W., Carrick, T.R., Willoughby, L.G.: Effects of diet, body size, age and temperature on growth rates in the amphipod Gammarus pulex. Freshwater Biology **11**(2), 183–214 (1981). DOI 10.1111/j.1365-2427.1981.tb01252.x

[57] Svensson, C., Baden, S., Moksnes, P.O., Aberg, P.: Temporal mismatches in predator-herbivore abundance control algal blooms in nutrient-enriched seagrass ecosystems. Marine Ecology Progress Series **471**, 61–71 (2012). DOI 10.3354/meps10014

[58] Tärnlund, S., Sundqvist, F.: Faktablad – Resultat från övervakningen av kustfisk 2016:5 Barsebäck (Öresund) 1999–2016. Tech. rep., Sveriges lantbruksuniversitet, Institutionen för akvatiska resurser (2016)

[59] Thompson-Svanfeldt, K., Looström, J., Käll, F.: Biologisk recipientkontroll för Ringhals kärnkraftverk. Aqua Reports **2022:7** (2022)

[60] Öresunds vattenvårdsförbund: Undersökningar | Öresunds vattenvårdsförbund (2024). URL `https://www.oresunds-vvf.se/undersokningar/`. Visited on 2024-05-31

[61] Virtanen, P., Gommers, R., Oliphant, T., Haberland, M., Reddy, T., Cournapeau, D., Burovski, E., Peterson, P., Weckesser, W., Bright, J., Walt, S., Brett, M., Wilson, J., Millman, K., Mayorov, N., Nelson, A., Jones, E., Kern, R., Larson, E., Pingel, T.: Scipy 1.0–fundamental algorithms for scientific computing in python. Nat Methods (2019). DOI 10.48550/arXiv.1907.10121

[62] Watson, G.S.: Smooth regression analysis. Sankhyā: The Indian Journal of Statistics, Series A **26**(4), 359–372 (1964)